

การออกแบบเพปไทด์ที่มีฤทธิ์ยับยั้งการเกิดโปรตีนเชิงซ้อนของ

Human papillomavirus 16 E1-E2



นายวรพล กันตัง

จุฬาลงกรณ์มหาวิทยาลัย

CHULALONGKORN UNIVERSITY

บทคัดย่อและแฟ้มข้อมูลฉบับเต็มของวิทยานิพนธ์ตั้งแต่ปีการศึกษา 2554 ที่ให้บริการในคลังปัญญาจุฬาฯ (CUIR)

เป็นแฟ้มข้อมูลของนิสิตเจ้าของวิทยานิพนธ์ ที่ส่งผ่านทางบัณฑิตวิทยาลัย

The abstract and full text of theses from the academic year 2011 in Chulalongkorn University Intellectual Repository (CUIR) are the thesis authors' files submitted through the University Graduate School.

วิทยานิพนธ์นี้เป็นส่วนหนึ่งของการศึกษาตามหลักสูตรปริญญาวิทยาศาสตรมหาบัณฑิต

สาขาวิชาชีวเคมีและชีววิทยาโมเลกุล ภาควิชาชีวเคมี

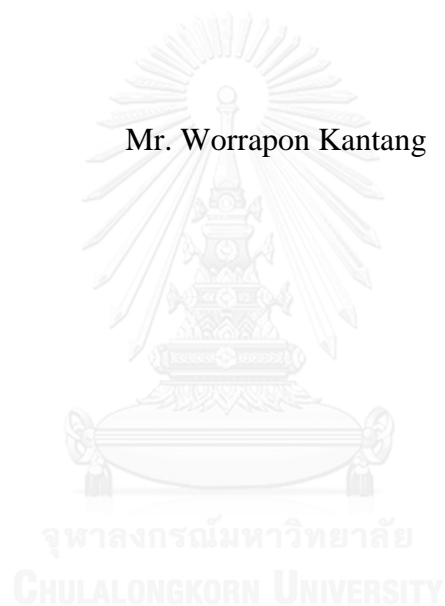
คณะวิทยาศาสตร์ จุฬาลงกรณ์มหาวิทยาลัย

ปีการศึกษา 2558

ลิขสิทธิ์ของจุฬาลงกรณ์มหาวิทยาลัย

DESIGNING PEPTIDES WITH INHIBITORY ACTIVITY ON
HUMAN PAPILLOMAVIRUS 16 E1-E2 PROTEIN COMPLEX FORMATION

Mr. Worrapon Kantang



A Thesis Submitted in Partial Fulfillment of the Requirements
for the Degree of Master of Science Program in Biochemistry and Molecular Biology
Department of Biochemistry
Faculty of Science
Chulalongkorn University
Academic Year 2015
Copyright of Chulalongkorn University

รพล กันตัง : การออกแบบเปปไทด์ที่มีฤทธิ์ยับยั้งการเกิดโปรตีนเชิงซ้อนของ Human papillomavirus 16 E1-E2 (DESIGNING PEPTIDES WITH INHIBITORY ACTIVITY ON HUMAN PAPILLOMAVIRUS 16 E1-E2 PROTEIN COMPLEX FORMATION) อ.ที่ปรึกษาวิทยานิพนธ์หลัก: ผศ. ดร. เกื้อการุณย์ คุรุสง, อ.ที่ปรึกษาวิทยานิพนธ์ร่วม: ดร. สุรศักดิ์ ชื่นศรีวิโรจน์, 100 หน้า.

อิวแมนปาปิลโลมาไวรัส 16 เป็นดีเอ็นเอไวรัสที่สามารถติดต่อกได้ในมนุษย์และเป็นสาเหตุของมะเร็งปากมดลูก โปรตีนเอชพีวี 16 E2 มีบทบาทสำคัญในการควบคุมและเพิ่มจำนวนยีนของไวรัส งานวิจัยของ Fujii และคณะปี 2003 รายงานว่า ได้ค้นพบเปปไทด์ 9 สายที่มีความสามารถในการจับกับเอชพีวี 16 E2 ด้วยเทคนิค phage display ในงานวิจัยนี้มีจุดมุ่งหมายที่จะคาดการณ์รูปแบบและปฏิสัมพันธ์ระหว่างเปปไทด์กับ เอชพีวี 16 E2 รวมถึงการออกแบบเปปไทด์ตัวใหม่ที่มีความสามารถในการจับกับเอชพีวี 16 E2 และยับยั้งการรวมตัวกันของ E1 กับ E2 เพื่อควบคุมการเพิ่มจำนวนยีนของไวรัส โดยใช้เทคนิคทางคอมพิวเตอร์ ในงานวิจัยนี้ ได้ทำการ Dock เปปไทด์ที่สร้างขึ้นกับ E2 โดยใช้ ClusPro Web Server พบว่า ผลการวิเคราะห์ความสามารถของการจับกันระหว่างเปปไทด์กับ E2 ทางคอมพิวเตอร์ มีความสอดคล้องกับผลการทดลองในระดับหลอดทดลอง โดยเปปไทด์ 4 สามารถจับกับ E2 ได้ดีที่สุด จึงออกแบบเปปไทด์สายสั้นๆ โดยใช้เปปไทด์ 4 (TWFWPYPYPLP) เป็นต้นแบบ โดยทริปโตเฟน ตำแหน่ง 4 ของเปปไทด์ 4 ถูกเปลี่ยนเป็น ฮิสทีดีน แอสพาราจินและเซอรัลีน ไทโรซีนตำแหน่งที่ 6 ของเปปไทด์ 4 ถูกเปลี่ยนเป็น ลิวซีน แอสพาราจินและอาจินิน เปปไทด์ที่ถูกออกแบบใหม่ 5 สายที่ให้ค่าพลังงานการจับกับ E2 ต่ำกว่าเปปไทด์ 4 ถูกนำไปสังเคราะห์ และนำไปใช้ในการทดสอบการจับกับ E2 ในระดับหลอดทดลอง ในงานวิจัยนี้ผลิตโปรตีนรีคอมบิแนนท์เอชพีวี 16 E1 และ E2 ใน *Escherichia coli* และทำให้บริสุทธิ์โดยใช้ Nickel column chromatography จากการวิเคราะห์การจับกันของเปปไทด์และ E2 ด้วยเทคนิค Enzyme-linked immunosorbent assay พบว่าเปปไทด์ Y6R, W4H_Y6R และ W4H สามารถจับกับ E2 ได้ดีกว่าเปปไทด์ 4 ต้นแบบ และเปปไทด์ทั้งสามชนิดนี้ ยังมีความสามารถในการยับยั้งการจับระหว่าง E1 กับ E2 ได้ดีกว่าเปปไทด์ 4 ต้นแบบ

ภาควิชา ชีวเคมี

ลายมือชื่อนิสิต

สาขาวิชา ชีวเคมีและชีววิทยาโมเลกุล

ลายมือชื่อ อ.ที่ปรึกษาหลัก

ปีการศึกษา 2558

ลายมือชื่อ อ.ที่ปรึกษาร่วม

5572097623 : MAJOR BIOCHEMISTRY AND MOLECULAR BIOLOGY

KEYWORDS: HPV16 / SMALL PEPTIDE INHIBITOR / E1 / E2 / CLUSPRO / DOCKING / I-TASSER

WORRAPON KANTANG: DESIGNING PEPTIDES WITH INHIBITORY ACTIVITY ON HUMAN PAPILLOMAVIRUS 16 E1-E2 PROTEIN COMPLEX FORMATION. ADVISOR: ASST. PROF. KUAKARUN KRUSONG, Ph.D., CO-ADVISOR: SURASAK CHUNSRIVIROT, Ph.D., 100 pp.

Human papillomavirus 16 (HPV 16) is a DNA virus that is capable of infecting humans and causing cervical cancer. HPV16 E2 plays an important role in viral gene regulation and replication. Fujii et al 2003 reported that nine peptides screened by phage display technique, could bind to HPV16 E2. This work aims to predict the binding conformations and interactions between the dodecapeptides and HPV16 E2 as well as to design novel peptide inhibitors that are capable of binding to HPV16 E2 and disrupting the transcriptional regulator E1-E2 complex formation, using computational protein design techniques. ClusPro Web Server was used to dock these peptides to E2. The ranking of the predicted binding affinities of the peptides is consistent to that of the experimental results; and peptide4 is the best E2 binder. Therefore, small peptides were designed based on peptide4 (TWFWPYPYPHLP). Trp4 of peptide4 was mutated to His, Asn and Ser, Tyr6 of peptide4 was mutated to Lys, Asn and Arg. Five newly designed peptides that showed lower binding energy to HPV16 E2 than that of peptide4, were selected for *in vitro* experiments. The HPV16 E1 and E2 were expressed and purified in *Escherichia coli*. Enzyme- linked immunosorbent assay was used to test whether the designed peptides could bind to HPV16 E2 and disrupt the E1-E2 complex formation better than peptide4. Y6R, W4H_Y6R and W4H peptides could bind better to HPV16 E2 than peptide4 did. Moreover, these three peptides are more effectively inhibited E1-E2 complex formation than peptide 4.

Department:	Biochemistry	Student's Signature
Field of Study:	Biochemistry and	Advisor's Signature
	Molecular Biology	Co-Advisor's Signature

Academic Year: 2015

ACKNOWLEDGEMENTS

This thesis would not have been completed without good suggestion from many people. I would like to express my deepest gratitude to my advisor Assistant Professor Dr. Kuakarun Krusong and my Co- advisor Dr. Surasak Chunsrivirod for their guidance, supervision, and supports throughout this thesis.

My gratitude is also extended to thesis committees, Associate Professor Dr. Rath Pichyangkura, Assistant Professor Dr. Kunlaya Somboonwiwat and Professor Dr. Wasun Chantratita for their valuable comments, and useful suggestion.

Thanks are expressed to all students and researchers of the Biochemistry Department and Biochemistry Program for their friendships and help in the laboratory.

I appreciate the financial support from Chulalongkorn University through the 90th Year Chulalongkorn Scholarship.

Finally, my greatest indebtedness is expressed to my parents and family members for their love, understanding, supporting and encouragement with care which have enable me to carry out this study successfully whereas I have spent most of my time with this thesis rather than with them.

CONTENTS

	Page
THAI ABSTRACT	iv
ENGLISH ABSTRACT.....	v
ACKNOWLEDGEMENTS	vi
CONTENTS.....	vii
LIST OF TABLES	xi
LIST OF FIGURES	xii
LIST OF ABBREVIATIONS.....	xiv
CHAPTER I.....	1
INTRODUCTION	1
1.1 General introduction.....	1
1.2 Epidemiology	2
1.3 Structure and function of HPV	3
1.4 Classification	6
1.5 HPV life cycle	7
1.5.1 Infectious entry.....	7
1.5.2 Viral persistence	7
1.5.3 Production of progeny virus	8
1.6 Clinical manifestations	9
1.6.1 Cutaneous warts	9
1.6.2 Epidermodysplasia verruciformis.....	10
1.6.3 Anogenital warts.....	10
1.6.4 Cervical cancer	11
1.7 Replication Initiation	13
1.7.1 The E1 protein	16
1.7.2 The E2 protein	17
1.7.3 The E1 and E2 complex	19
1.8 Anti-viral replication therapies.....	21
1.9 Prevention and treatment	22

	Page
1.10 Objective of the dissertation	23
CHAPTER II.....	24
MATERIALS AND METHODS.....	24
2.1 Materials	24
2.1.1 Equipments.....	24
2.1.2 Chemicals and reagents	25
2.1.3 Enzymes	28
2.1.4 Bacterial strains	28
2.1.5 Experiment kits.....	28
2.1.6 Vectors.....	28
2.1.7 Softwares	28
2.2 Prediction of HPV16 E1-E2 interactions, binding conformations and interactions between the peptides and HPV16 E2.....	29
2.3 Design of peptides to inhibit HPV16 E1-E2 complex.....	30
2.4 Expression and purification of recombinant of HPV16 E1.....	31
2.4.1 Construction of the recombinant E1-pMAL-c5x	31
2.4.2 Primer design.....	33
2.4.3 PCR conditions.....	33
2.4.4 Plasmid DNA extraction	34
2.4.5 Plasmid DNA preparation	35
2.4.6 E1 gene fragment preparation	35
2.4.7 Purification of DNA fragments	36
2.4.8 Determination of the quantity and quantity of DNA samples.....	36
2.4.9 Ligation of vector DNA and the E1 gene fragment	37
2.4.10 <i>E.coli</i> competent cell preparation	37
2.4.11 Transformation	38
2.4.12 Expression of HPV16 E1 gene	38
2.4.13 Purification of recombinant HPV16 E1	39
2.5 Expression and purification of recombinant of HPV16 E2.....	39

	Page
2.5.1 Construction of the recombinant of E2-pET28b(+)	39
2.5.2 Primer design	41
2.5.3 PCR conditions	41
2.5.4 Plasmid DNA preparation	42
2.5.5 E2 gene fragment preparation	42
2.5.6 Ligation of vector DNA and the E2 gene fragment	43
2.5.7 Expression of HPV16 E2 gene	43
2.5.8 Purification of recombinant HPV16 E2	43
2.6 Protein analysis	44
2.6.1 SDS-PAGE	44
2.6.2 Western blot analysis	45
2.7 Binding assays	47
2.7.1 Binding of HPV16 E1 and E2	47
2.7.2 Binding of designed peptides to HPV16 E2	48
2.7.3 Determination of the inhibitory concentration 50% (IC ₅₀) of designed peptides that disrupt E1-E2 binding	48
CHAPTER III	50
RESULTS	50
3.1 Structural similarity between HPV16 and HPV18 E1-E2 complexes	50
3.2 Analysis of HPV16 E1-E2 interactions	52
3.3 Construction of the peptides structures using I-TASSER	54
3.4 Design of peptides to inhibit HPV16 E1-E2 complex	58
3.5 Cloning, expression and purification of HPV16 E1	64
3.5.1 Construction of E1-pMAL-c5x	64
3.5.2 Expression of recombinant E1-pMAL-c5x	66
3.5.3 Purification of the recombinant E1-pMAL-c5x	67
3.6 Cloning, expression and purification of HPV16 E2	68
3.6.1 Construction of E2-pET28b(+)	68
3.6.2 Expression of recombinant E2-pET28b(+)	70

	Page
3.6.3 Purification of the recombinant E2/pGET28b(+)	71
3.7 Binding assays	72
3.7.1 Binding of HPV16 E1 and E2	72
3.7.2 Binding of designed peptides to HPV16 E2	74
3.7.3 Determination of the inhibitory concentration 50% (IC ₅₀) of designed peptides that disrupt E1-E2 binding	76
CHAPTER IV	79
DISCUSSION	79
CHAPTER V	86
CONCLUSIONS	86
REFERENCES	88
VITA	100



LIST OF TABLES

Table 1 A description of the function of HPV open reading frames	6
Table 2 HPV type and disease association	11
Table 3 The Bethesda classification system for cervical squamous cell dysplasia	13
Table 4 List of primers used for amplification of HPV16 E1 gene (residue 421-622)	33
Table 5 PCR conditions for amplification of HPV16 E1 gene (residue 421-622)	34
Table 6 List of primers used for amplification of truncated HPV16 E2 gene (residues 1-201)	41
Table 7 PCR conditions for amplification of HPV16 E2 gene (residues 1-201)	42
Table 8 The best structures and the C-scores of the nine peptides constructed by I-TASSER	55
Table 9 The lowest binding energies of the largest clusters (the best binding conformations) of the peptides to HPV16 E2, compared to their experimental A values	57
Table 10 The lowest binding energies of the largest clusters of the designed peptides inhibitors targeting HPV16 E2	62
Table 11 Properties of peptide inhibitors	78

LIST OF FIGURES

Figure 1 Map of HPV16 genome.....	5
Figure 2 The HPV life cycle	9
Figure 3 Transformation zone of the vagina.....	12
Figure 4 Model of the initiation replication on the ori.....	15
Figure 5 Crystal structure of DNA binding domain and helicase domain of E1	17
Figure 6 Crystal structure of transactivation domain and DNA binding domain of E2	19
Figure 7 Structure of the E1/E2 complex (helicase domain of E1 and transactivation domain of E2).....	20
Figure 8 Map of pMAL-c5x	32
Figure 9 Map of pET28b(+).	40
Figure 10 Exploded view of the Trans-Blot Module (Bio-RAD).....	46
Figure 11 Superimposition of the predicted HPV16 E1-E2 and HPV18 E1-E2 complexes	51
Figure 12 Analysis of HPV16 E1-E2 interactions. (A) Structure of the predicted HPV16 E1-E2 complex.	53
Figure 13 Docking of HPV16 E2 and nine peptides.....	56
Figure 14 Binding conformation and interactions of peptide4, the best E2 binder, within HPV16 E1-E2 interface	59
Figure 15 Design of peptides to disrupt interactions between HPV16 E1 and E2 by mutating TRP4 of peptide4.....	60
Figure 16 Design of peptides to disrupt interactions between HPV16 E1 and E2 by mutating TYR6 of peptide4	61
Figure 17 Binding conformations and interactions of designed peptides within HPV16 E1-E2 interface	63
Figure 18 Analysis of recombinant E1-pMAL-c5x plasmid by <i>NcoI</i> - <i>EcoRI</i> digestion.....	64
Figure 19 The blastX program showed that recombinant E1-pMAL-c5x plasmid has highest similarity to HPV16 E1 with 100% identity.	65
Figure 20 Expression level of recombinant HPV16 E1 protein.	66

Figure 21 Purification and Western blot analysis of E1-pMAL-c5x.....	67
Figure 22 Analysis of recombinant E2-pET28b plasmid by <i>XhoI-EcoRI</i> digestion....	69
Figure 23 The blastX program showed that recombinant E2-pET28b(+) has highest similarity to HPV16 E2 with 100% identity	69
Figure 24 Expression level of recombinant HPV16 E2 protein	70
Figure 25 Purification and Western blot analysis of E2-pET28b(+)	71
Figure 26 Quantitative binding of recombinant HPV16 E1 and E2	73
Figure 27 Quantitative binding of peptides and recombinant HPV16 E2	75
Figure 28 Concentration-response curves of peptides that inhibit E1-E2 binding. Inhibitory activity of peptide4	77



LIST OF ABBREVIATIONS

bp	Base pair
BPV	Bovine papillomavirus
DBD	DNA-binding domain
C °	Degree Celcius
DNA	Deoxyribonucleic acid
et al	Et alii
HD	Helicase domain
HPV	Human papillomavirus
hr	Hour
IgG	Immunoglobulin G
kDa	Kilodalton
LCR	Long control region
M	Molar
MBP	Maltose binding protein
min	Minute
ml	Millilitre
mM	Millimolar
NLS	Nuclear localization signal
nm	Nanometre
OD	Optical density
ORF	Open reading frames
Ori	Origin of replication
PCR	Polymerase chain reaction
rpm	Round per minute
TAD	Transactivation domain
µg	Microgram
µl	Microliter
µM	Micromolar

CHAPTER I

INTRODUCTION

1.1 General introduction

Cervical cancer is the second most common cancer in women worldwide. It is the fourth-most common cause of death from cancer in women (de Sanjose et al., 2007). There are various medical advances in diagnosis, research and treatment but this disease mortality is still high in developing countries. In 2012, an estimation of cervical cancer occurred 528,000 new cases and 266,000 deaths from cervical cancer (Van Krieking et al., 2014). In Thailand, the estimated numbers of new cases and deaths from cervical cancer were 9,999 and 5,216, respectively (Ferlay et al., 2010). In developing countries, there are lack of awareness in this disease, limited access to screening and preventing that cause a high rate of death from cervical cancer (Bosch et al., 2008, Chan et al., 2010).

Human papillomavirus (HPV) has been determined as one of the most important cause of development of cervical cancer. HPV infection is associated benign tumors (genital warts and respiratory, laryngeal papillomatosis), malignant lesions of the differentiating epithelium and causing cervical cancer with a variety of clinical conditions. Cervical cancer normally develops from precancerous changes over 10 to 20 years. About 90% of cervical cancer are squamous cell carcinomas, 10% are adenocarcinoma and other types (Shah and Buscema, 1988, Munoz et al., 2003, Cubie, 2013).

HPV is a small, double stranded DNA virus. To date, more than 170 different HPV types have been cataloged (Bernard et al., 2010). These viruses are classified depending on whether they cause benign warts or lesions that can progress to invasive cancer. There are considered as low-risk types if they cannot cause cervical cancer. Low-risk types usually cause genital warts or minor cell changes on the cervix and most of them HPV6 and 11 (de Villiers, 2013, de Villiers et al., 2004). In contrast, the viruses are considered as high-risk types if they are strongly associated with premalignant and malignant cervical lesions, mostly caused by HPV16 and 18 (Schlegel et al., 1988, Walboomers et al., 1999).

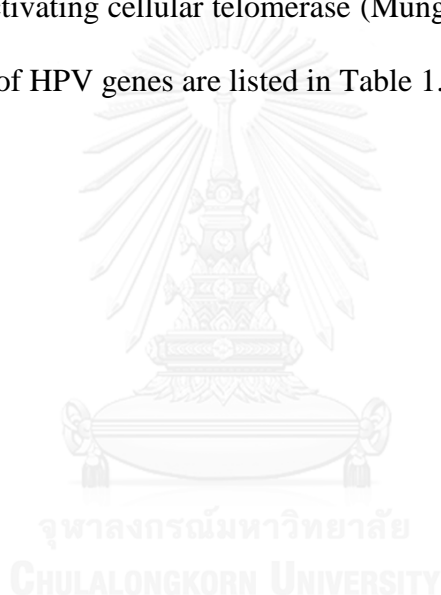
1.2 Epidemiology

Worldwide prevalence survey of HPV types has found 99.7% of cervical cancer specimens. HPV type16 was the most prevalent (54.6%), followed by HPV type18 (11%), HPV type45 (4.4%) and HPV type31 (3.4%). The prevalence of HPV was found in normal women (1.6% of low-risk and 13% of high-risk HPV types) (Rosenblatt et al., 2004). In addition, the prevalence of HPV types were found in differences countries, such as the detection rate of HPV16 in Asian and African was lower than detection rate in Europe. The U.S.A and Germany studies showed a higher prevalence of HPV16 and HPV18, but a lower prevalence of HPV52. Japanese studies showed a higher prevalence HPV52 and HPV58 but a lower prevalence of HPV16 and HPV18. In Thailand, HPV type16 was the most prevalent type (44.04%), followed by HPV type18 (15%), HPV type33 (9.33%) and HPV type11 (4%) (Siritantikorn et al., 1997, Watts et al., 2002).

1.3 Structure and function of HPV

HPV belongs to *Papillomavirus* genus of the family *Papovaviridae*. The virus is a small non-enveloped DNA virus. The genome contains circular double-stranded DNA of approximately 8 kb, associated with histone-like proteins and protected by a capsid with icosahedron symmetry. All of the open reading frames (ORFs) of the genomes are located on one strand. The ORFs are divided into three regions (long control region, early region, late region) (Figure 1). The long control region (LCR), is a short DNA sequence motifs size ranges between 7-10% of total genome. This region are recognized and bound by many transcriptional regulatory factor such as binding site for the transcription factor Sp1, binding sites for the viral factor E2, and a TATA box (Stunkel and Bernard, 1999, Bernard, 2013). The second region is early region (E), that contains six open reading frames (E1, E2, E4, E5, E6, and E7). The third is late region (L) that encodes the L1 and L2 structural proteins. The E1 protein represented ATPase and helicase activity, which functions to promote viral replication. The E2 protein increases the affinity of E1 to binding to the viral replication region. Appearance of both E1 an E2 is necessary to induce viral DNA replication (Brentjens et al., 2002, Sanclemente and Gill, 2002). Furthermore, E2 protein has an important role in both viral transcription activator and repressor by interacting with transcription factors such as TFIIB, SP1 (Tan et al., 1994, Rank and Lambert, 1995, Thierry, 2009). HPV E4 function is unclear. Perhaps, it is associated with collapse of the cellular cytokeratin network and enhances virus exit from the cell host (Raj et al., 2004, Wilson et al., 2005). E5 protein enhances the transforming activity of E6 and E7 (Alonso and Reed, 2002). E6 and E7 enable HPV to use cellular proteins for continuing viral replication. Both proteins have been shown to inhibit the function of the tumor suppressor protein p53

and pRb (retinoblastoma protein) (Turek, 1994, Yim and Park, 2005). E6 has multiple roles in the cell and interacts with many proteins. Its major function is to degrade of p53, a major tumor suppressor protein, reducing the ability of cell to respond to DNA damage. E7 protein inactivates members of the pRb family of tumor suppressor proteins. Rb plays an important regulatory role in cell division. Presence of protein E6 and E7 serves to prevent cell death (apoptosis) and promote cell cycle progression, thus priming the cell for replication of the viral DNA. E7 also participates in immortalization of infected cells by activating cellular telomerase (Munger et al., 1992, Yim and Park, 2005). The functions of HPV genes are listed in Table 1.



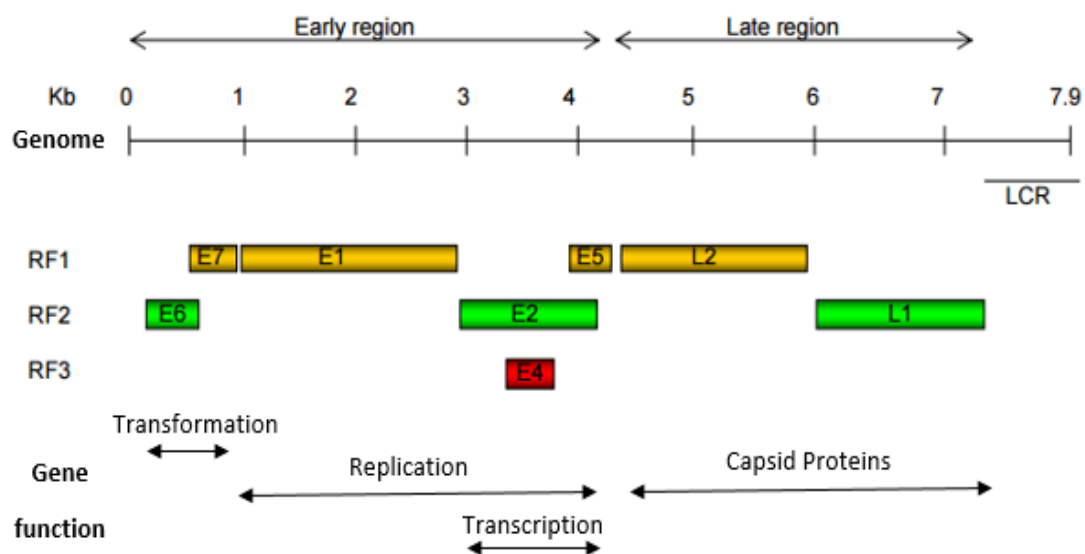


Figure 1 Map of HPV16 genome. The viral genes are transcribed in a single direction. There are genes coding for non-structural proteins (E1, E2, E4, E5, E6, and E7) and structural proteins (L1, L2), and a transcriptional control region (long control region; LCR). LCR contains a DNA replication origin and functions as the regulator for the DNA replication (Kajitani et al., 2012).

Table 1 A description of the function of HPV open reading frames (Sancllemente and Gill, 2002).

Protein	Functions
E1	DNA helicase activity, DNA-dependent ATP-binding, ATPase activity. Role in viral DNA replication.
E2	Controls viral transcription, DNA replication, and necessary for viral DNA replication together with E1.
E4	Supports the HPV genome amplification, regulates the expression of late genes, helps the release of virions.
E5	Enhances the transforming activity of E6 and E7.
E6	E6 of high-risk HPVs degrades the tumor-suppressor protein p53, inhibits apoptosis, activates the expression of telomerase. Together with E7 provides a cellular environment for viral DNA replication.
E7	Degrades the tumor-suppressor protein pRb resulting in expression of S-phase of cell cycle by directly interacting with E2F factor. Induces a peripheral tolerance in cytotoxic T lymphocytes. Downregulates the expression of TLR9, contributing to immune response evasion.
L1	Major capsid protein.
L2	Minor capsid protein.

1.4 Classification

The classification of HPV is related to degree of genomic properties. HPV type is classified by having less than 90% nucleotide sequence homology within the L1 open reading frame (ORF) of all other known types, subtypes have DNA homology between 90% - 95% (de Villiers et al., 2004). To date, more than 170 human papillomavirus types have been completely identified (zur Hausen, 2000). These viruses are classified based on their potential for malignant transformation. Low risk types such as HPV6, 11, 42, 43, 44 are associated with anogenital warts. High risk types such as HPV16, 18,

31, 33, 35, 39, 45, 51, 52, 56, 58, 66 are associated with premalignant and malignant cervical lesions. In 1995, IARC (International Agency for Research on Cancer) evaluated all relevant data on the carcinogenicity of HPV and concluded that there was sufficient evidence to categorize HPV type 16 and 18 as human carcinogens (Walboomers et al., 1999).

1.5 HPV life cycle

1.5.1 Infectious entry

The HPV enter to keratinocyte stem cells through small wounds in the skin or mucosal surface. The virus can get inside from the cell surface via interaction with a specific receptor such as alpha-6 integrin, heparan sulfate proteoglycans (HSPGs) and transported to membrane-enclosed vesicles called endosomes. The capsid protein L2 disrupts the membrane of the endosome, allowing the viral genome to escape and traffic, along with L2, to the cell nucleus (Sapp and Bienkowska-Haba, 2009, Horvath et al., 2010).

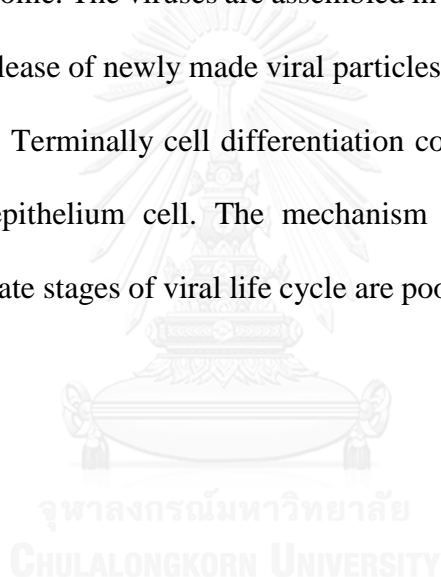
1.5.2 Viral persistence

After the viral successful infection, E1 and E2 proteins are expressed. These proteins are expressed for replicating and maintaining the viral DNA as a circular episome (Stubenrauch and Laimins, 1999). The cell containing the episome begins its differentiation process, a subset of differentiation-dependent viral promoters is also activated and other viral proteins are made. Although differentiate cells do not normally replicate their DNA, the E6 and E7 force the cell to produce the elements that necessary for DNA replication and provide the needed environment for viral amplification. The

viral oncogenes E6 and E7 promote cell growth by inactivating the tumor suppressor proteins p53 and pRb, respectively (Longworth and Laimins, 2004, McKinney et al., 2015).

1.5.3 Production of progeny virus

The viral late genes L1 and L2 were expressed in the outermost layers of mucosal surface. The expression of L1 and L2 were correlated with the number of copies of the viral genome. The viruses are assembled in the cell nucleus. HPVs are not lytic viruses, as the release of newly made viral particles does not occur through active disruption of the cell. Terminally cell differentiation containing newly viral particles are shed from the epithelium cell. The mechanism of viruses released into the environment and the late stages of viral life cycle are poorly understood (Meyers et al., 2002).



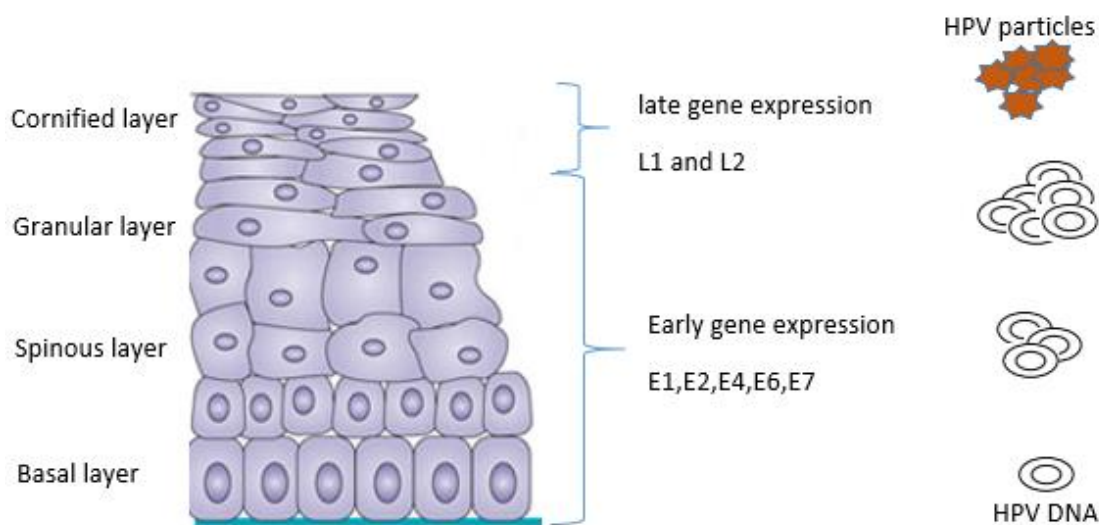


Figure 2 The HPV life cycle. The initial infection occurs through micro lesion of epithelium cell from the basal layer. As the host cell differentiates and migrates to lumen of the cervix, viral proteins are expressed and viral DNA is amplified. In cell going to terminal differentiation, the capsid protein are produced and viral particles assembled (Liu et al., 2001).

1.6 Clinical manifestations

The HPV that causes a various of disease depend on HPV type (Table 2). High-risk HPVs may lead to the development of cervical cancer. Low-risk HPVs may lead to cutaneous warts epidermodysplasia verruciformis and anogenital warts.

1.6.1 Cutaneous warts

Three major types of cutaneous warts are identified; deep plantar warts, common wart, and flat wart. Deep plantar warts are usually small solitary lesions especially located on soles of feet and toes. Common warts are small, grainy skin

growth often occur on the fingers or hand. Flat warts present as multiple, small, flat, smooth papules with pink to tan colour occur on face, neck, legs, hands and fingers of children (Brentjens et al., 2002).

1.6.2 Epidermodysplasia verruciformis

Epidermodysplasia verruciformis (EV) is characterized by the appearance of flat wart-like lesions, red to brown plaques. HPV genotypes associated with EV have been observed in patients who are immunosuppressed or in patients with HIV infection. Over 20 different HPV types have been isolated from EV lesion (Table 2) (Brentjens et al., 2002).

1.6.3 Anogenital warts

Anogenital warts or genital warts are the most commonly recognized clinical lesion of HPV infection. Anogenital warts may occur singly but are more often found in clusters. In men, the warts usually develop on the outer skin of the penis. In women, the warts often develop on the vulva to outside the vagina. The most anogenital warts are caused by HPV types 6 or 11 (Brentjens et al., 2002).

Table 2 HPV type and disease association (Brentjens et al., 2002).

Disease	HPV types	
	Frequent association	Less-frequent association
Deep plantar warts	1, 2	4, 63
Common warts	1, 2, 7	4, 26, 27, 29, 57, 65 26, 27, 28, 38, 75, 76
Flat warts	3, 10	
Epidermodysplasia verruciformis	2, 3, 10, 5, 8, 9, 12, 14, 15, 17	19, 20, 21, 22, 23, 24, 25, 36, 37, 38, 47, 50
Condyloma acuminata (genital warts)	6, 11	30, 42, 43, 45, 51, 54, 55, 70
Intraepithelial neoplasia (IN) Unspecified	-	30, 34, 39, 40, 53, 57, 59, 61, 62, 64, 66, 67, 68, 69
Low grade	6, 11	16, 18, 31, 33, 35, 42, 43, 44, 45, 51, 52, 74
High grade	16, 18	6, 11, 31, 34, 33, 35, 39, 42, 44, 45, 51, 52, 56, 58, 66
Cervical carcinoma	16, 18	31, 45, 33, 35, 39, 51, 52, 56, 58, 66, 68, 70
Anogenital warts	6, 11	

1.6.4 Cervical cancer

Cervical cancer is defined by abnormal growth of cell at the cervix and can invade or spread to other parts of the body. At early stage, typically no symptoms are seen. Later symptoms may include abnormal vaginal bleeding, pelvic pain, or pain during sexual intercourse. HPV is the main factor of cervical cancer (Clifford et al., 2005, Munoz et al., 2006, Zekri et al., 2006). Worldwide, specific types of HPV are types 16 and 18 that cause cervical cancer. All cervical cancer develop in the transformation zone that is located at the stratified squamous epithelium of the vagina (Burd, 2003).

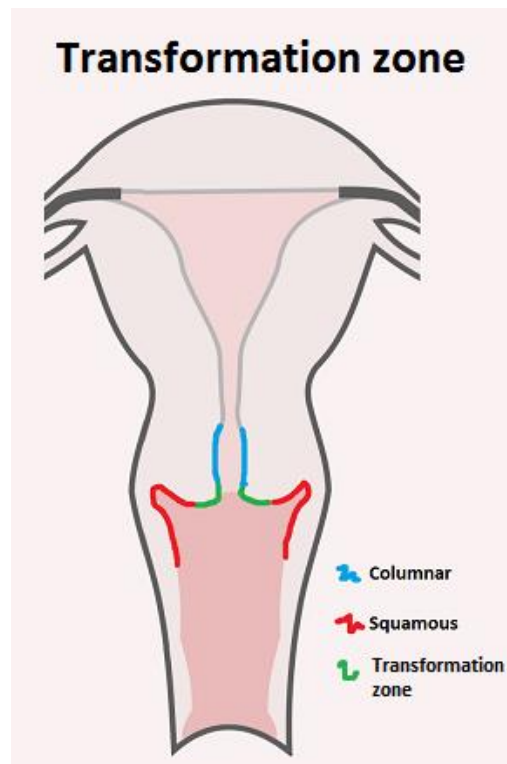


Figure 3 Transformation zone of the vagina (Source: <http://almostadoctor.co.uk>)

The classification of abnormalities of the cervical epithelium is based on CIN system (Cervical intraepithelial neoplasia). These abnormalities are classified as CIN I, II, III (Table 3) (Pinto and Crum, 2000). The Bethesda system, developed at the United States National Cancer Institute, is more appropriate for use in cytological reports (Montz, 2000). The Bethesda system classifies abnormalities squamous cell into 4 categories, atypical squamous cells (ASC), low grade squamous intraepithelial lesion (LGSIL or LSIL), high grade squamous intraepithelial lesion (HGSIL or HSIL), and squamous cell carcinoma or adenocarcinoma. In addition, the ASC category consist of two subcategories: atypical squamous cells of undetermined significance (ASC-US) and atypical squamous cells, cannot exclude HSIL (ASC-H) (Table 3) (Jones, 2000, Zuna et al., 2002).

Table 3 The Bethesda classification system for cervical squamous cell dysplasia

(Jones, 2000, Zuna et al., 2002).

Pap test	Bethesda System	CIN System
Class I	Normal	Normal
Class II	ASC-US, ASC-H	
Class II	LSIL	CIN 1 including flat condyloma
Class III	HSIL	CIN 2
Class III	HSIL	CIN 3
Class IV	HSIL	CIN 3
Class V	Invasive carcinoma	Invasive carcinoma

1.7 Replication Initiation

Initiation of HPV's DNA replication requires the replication origin that contains the E1 and E2 binding site, the viral E1 and E2 proteins. E1 is the primary replication protein. This protein is ATP-dependent helicase that specifically binds, melts and unwinds the viral replication origin to allow access of the replication. Only E1 can binding to the replication origin and drive papillomaviruse DNA replication but low affinity (Dixon et al., 2000, Titolo et al., 2003). The E2 act as a molecular tether to recruit the E1 to specifically at E1 binding site (E1BS) in the replication origin. Initially, E2 bind to the E1 binding site (E2BS) at the origin and recruits the E1. E1 and E2 are form E1/E2 complex at the replication origin. The E1/E2 complex acts as a template for the assembly of an E1 double hexamer to unwinding activity. Then, E1 changes conformation by binding to ATP, leading to release of E2 from the origin (Woytek et al., 2001). The E1 assembles into double trimers to unwind double-stranded DNA. The E1 double trimers function as precursors to form double hexamer of E1 that finally

function as a DNA helicase at replication forks. The E2 can be divided into two domains that are involved in directing E1 to the origin; first, DNA binding domain is high affinity interaction with E2BS in the origin. The second is transactivation domain that act as specifically to binding to E1 (Chen and Stenlund, 1998). The interaction not only helps to recruit E1 to the origin but also inhibits non-specific binding of the E1 to DNA. The interaction of E1/E2 is important role in the initiation of HPV DNA replication. So, it is a candidate to design an antiviral drug (Bergvall et al., 2013).



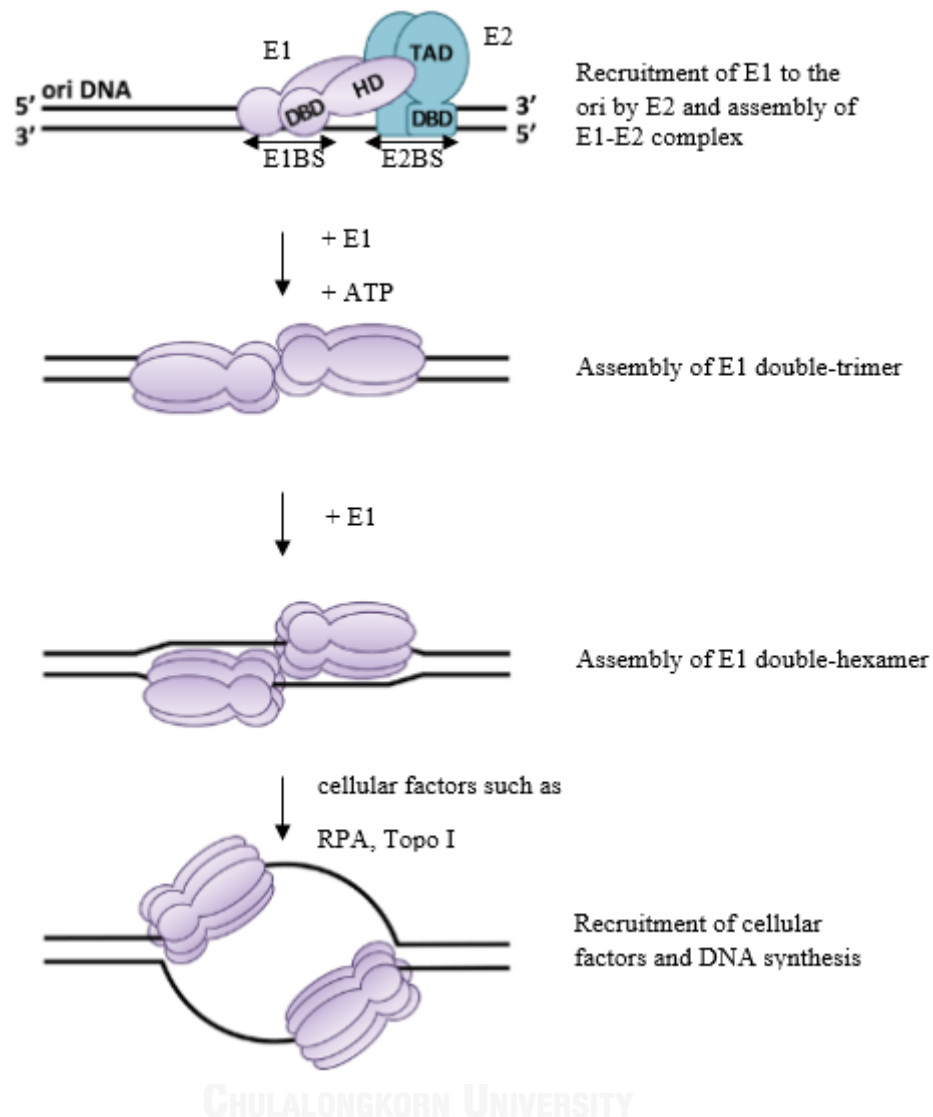


Figure 4 Model of the initiation replication on the ori. Replication is initiated by the recruitment of E1 (light purple) by E2 (light blue), to the ori and form E1-E2 complex. This complex serves as a template for the recruitment of additional E1 molecules and assembly of the E1 double-trimer. E1 double-trimer is converted into a double-hexamer in which each of the two hexamers encircles a separate DNA strand. This complex is capable of DNA unwinding and likely a platform for the recruitment of the cellular DNA replication factors (Bergvall et al., 2013).

1.7.1 The E1 protein

The E1 is encoded by the most conserved open reading frame (ORF) of papillomaviruse genome. This protein ranges in size from 600 – 650 amino acids depending on the PVs type (Morin et al., 2011). The E1 can be divided into three segment; an N-terminal regulatory region, a central origin-binding domain (known as the DNA-binding domain, DBD), and a C-terminal enzymatic domain or helicase domain (HD). The N-terminal region of E1, approximately 200 amino acids, consists of short amino acid sequence motifs, including nuclear localization signal (NLS) (Amin et al., 2000). This region is variably conserved amongst different PVs type. The DNA-binding domain recognizes specific sequences in the ori. The E1 binding to this region was characterized as a 18-nucleotide AT-rich imperfect palindrome which contains six E1-binding site (E1BS 1-6) of the consensus sequence 5'-ATTGTT-3'. The bovine papillomavirus1 (BPV1) E1 was used to model a structure (Figure 5B). The BPV1 E1 DBD consist of a central five stranded β -sheet, 4 α -helices on one side (α_1 , α_2 , α_5 , α_6) and 2 α -helices on the other side (α_3 , α_4). DNA binding loop of DBD that located between α_2 and β_1 has a key residues for DNA binding (Auster and Joshua-Tor, 2004). The helicase domain functions as DNA unwinding activity. In the crystal structure of BPV1 E1 hexamer, the six oligomerization domains form a rigid collar to the ATP-binding site (Figure 5C, B) (Amin et al., 2000).

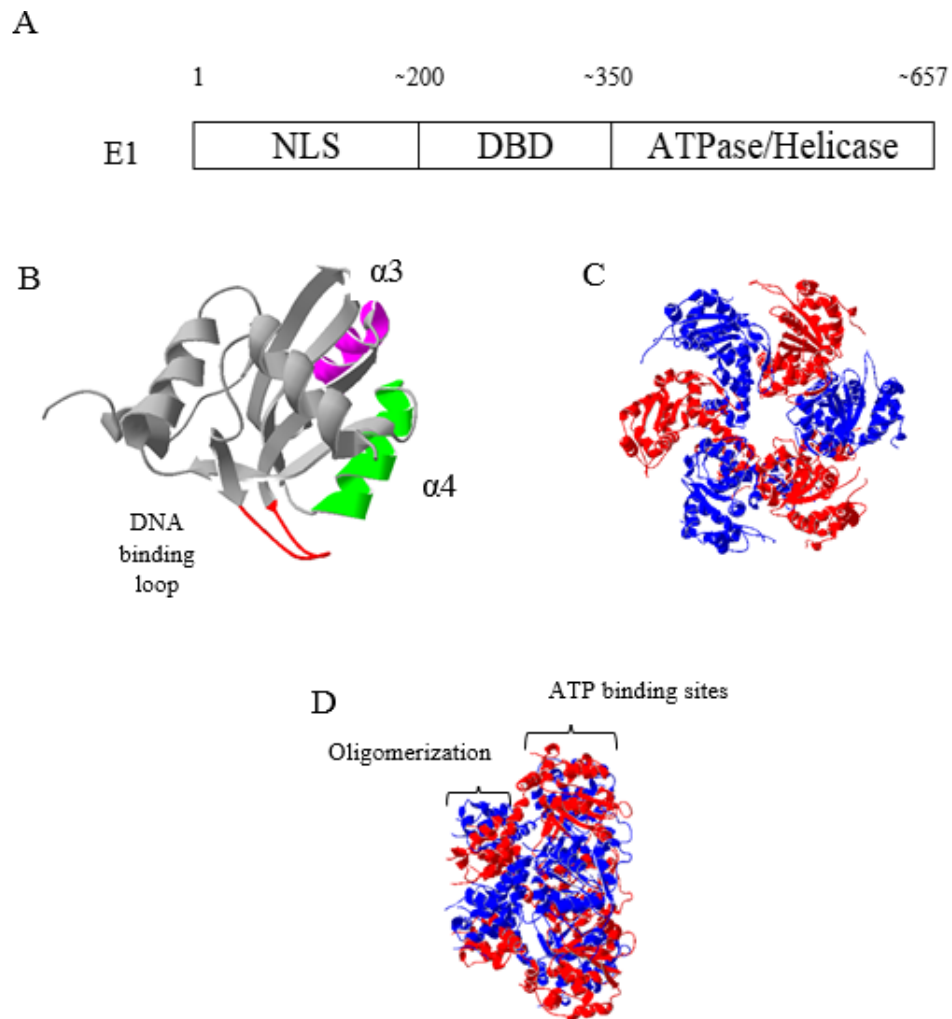


Figure 5 Crystal structure of DNA binding domain and helicase domain of E1 (A) Amino acid sequence E1. (B) Crystal structure of the BPV1 E1 DBD highlighting DNA-binding loop (PDB: 1R9W) (red), DNA binding helix ($\alpha 4$, green) and dimerization helix ($\alpha 3$, pink). Crystal structure of the BPV1 E1 HD front view (C) and side view (D). The six monomer are colored in blue and red (PDB: 2V9P) (Sanders et al., 2007).

1.7.2 The E2 protein

The HPV E2 protein is important for the viral life cycle. This protein functions as transcriptional regulation, initiation of DNA replication and partitioning the viral

genome (McBride, 2013). The E2 protein is encoded by the entire E2 open reading frame. The E2 protein can be divided into three domains: the N-terminal transactivation domain, the C-terminal DNA binding domain, and the hinge region between these domains (Figure 6). The transactivation domain contains a conserved sequence about 200 amino acids. The N-terminal half of this domain is composed of three alpha helices folded anti-parallel to each other (Amin et al., 2000, Abbate et al., 2004, Wang et al., 2004). The C-terminal half of domain is composed of mostly of anti-parallel beta sheet (Narechania et al., 2005). The center of these two transactivation domain is consist of a two turn helix. Residues within the transactivation domain are important for transcription activation and repression, and replication. For example, E39 is important for replication and interaction with the E1 protein (McBride, 2013). The DNA binding domain is responsible for homodimerization and binding to DNA (Kim et al., 2000). This domain forms a novel dimeric, eight-stranded, anti-parallel beta-barrel structure and two alpha helices on the surface of the barrel. The hinge is unstructured and forms a flexible link between the transactivation domain and DNA binding domain (Sekhar et al., 2010).

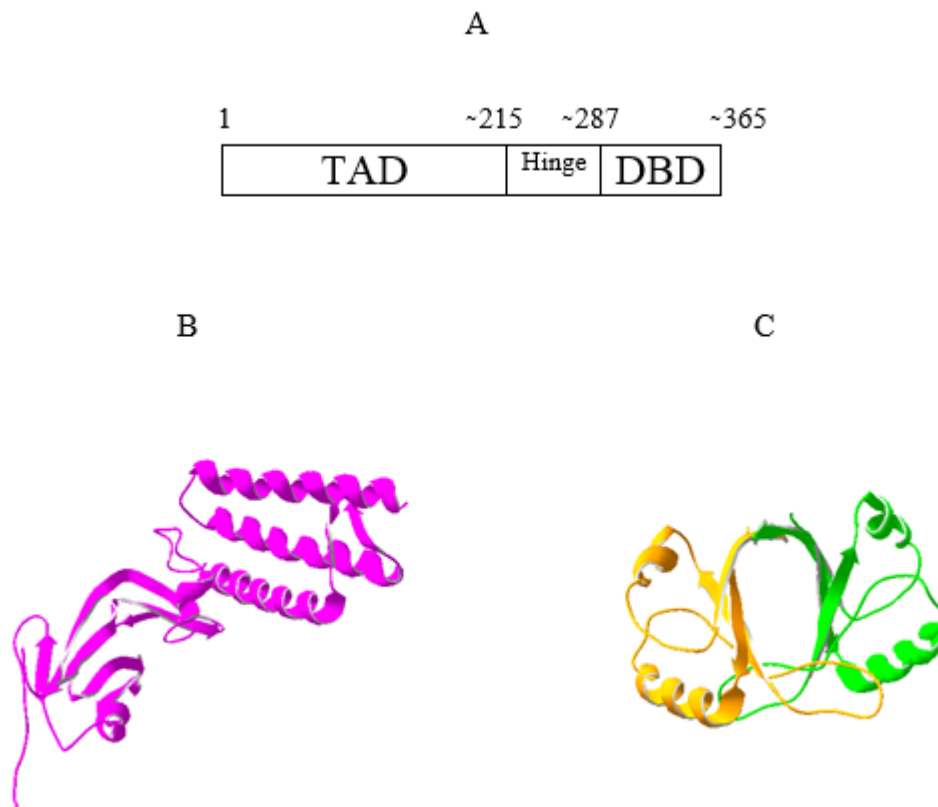


Figure 6 Crystal structure of transactivation domain and DNA binding domain of E2 (A) The Amino acid sequence E2. (B) Crystal structure of the HPV16 E2 transactivation domain is colored in pink (PDB: 1DTO). (C) Homodimerization of DNA binding domain of the HPV16 E2 are colored in orange and green (PDB: 1ZZF) (Antson et al., 2000).

1.7.3 The E1 and E2 complex

The E1/E2 complex is characterized by C-shaped structure. The E2 activation domain is formed at the top and side of C-shaped structure. The bottom of C-shape is formed by E1 helicase domain (Figure 7). The E2 activation domain consists of a α -helical N-terminal domain that is linked to the C-terminal β -strand domain by the linker segment. The E1 core is predominantly globular and has long loop extend out from the

core at either end. The major contact of E2 at E1/E2 complex are three helices of the N-terminal domain. The linker segment of E2 consisting of short anti-parallel β -strand between helices α B and α C are also mark contacts with E1. The major contact surface of E1 is formed by a bundle of helices comprising α 2, α 3, and α 9. E1 also makes additional contacts to E2 through a long extended loop between β 7 and α 9 (loop2, Figure 7) (Abbate et al., 2004).

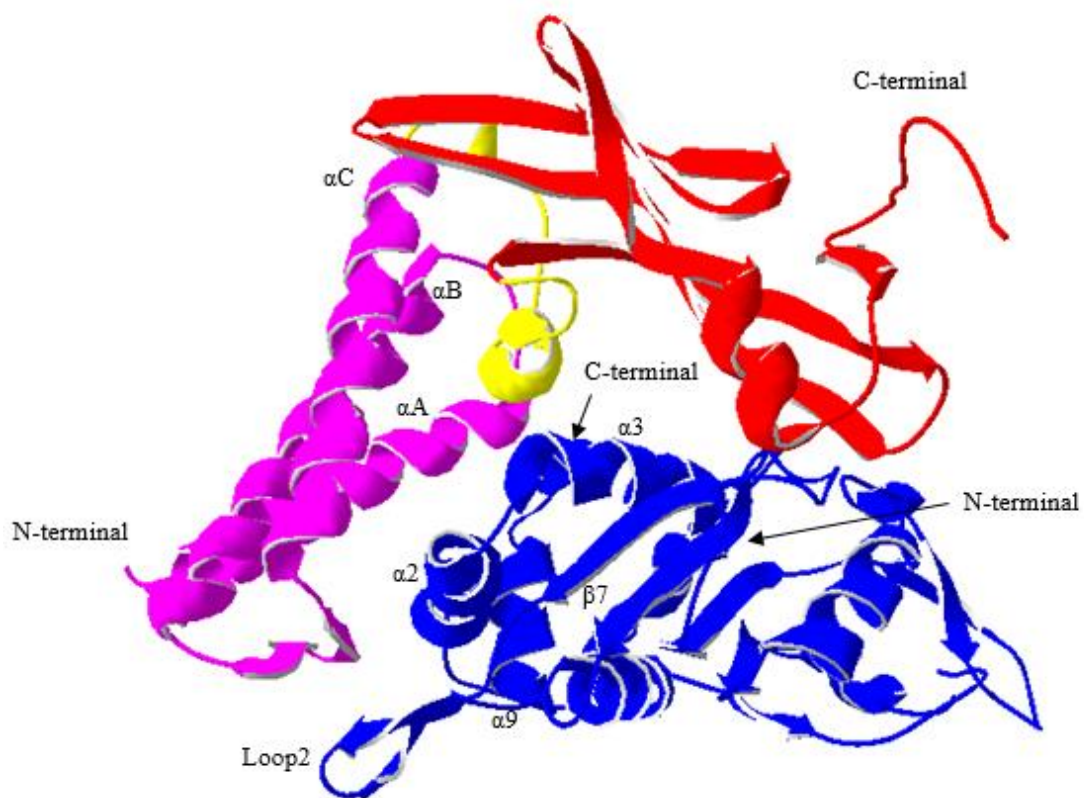


Figure 7 Structure of the E1/E2 complex (helicase domain of E1 and transactivation domain of E2). N-terminal helical domain of E2 is colored pink, the β -strand structural domain is colored red, and linker segment between the two domains of E2 is colored yellow. E1 is colored blue (PDB: 1TUE chain D of E1 and chain E of E2).

1.8 Anti-viral replication therapies

Although preventive HPV vaccines have been developed, they may not be capable of treating established HPV infections. Thus, it is crucial to develop therapeutic agents for controlling HPV infection. Most research has focused on the replication proteins to design antiviral drugs for HPV-associated diseases. White et al, 2003 designed a small molecule indandione to disrupt interaction between the N-terminal domain of E2 and the helicase domain of E1, in order to inhibit HPV-11 replication. Indandione was determined to binding to the TAD domain of E2, the same region of the protein that interacts with E1. Indandione induce movement of several amino acid side chains at the binding site of E2. These changes the side chain conformation of Tyr19, His32, Leu94, and Glu100. Schaal et al, 2003 designed hairpin polyamides to inhibit specific E1 and E2 DNA binding function. Hairpin polyamides consist of three N-methylpyrrole rings that led to the incorporation of novel heterocycles and chemical moieties paired with alternate structural motifs such as hairpins. Hairpin polyamides can bind to E2 homodimer and inhibit E2 function. Another attractive target is the enzymatic activities of the E1 ATPase/helicase that was used for inhibitors (D'Abramo and Archambault, 2011). Fujii et al, 2003 reported small peptides that could bind to HPV16 E2 from phage display library. Some of these peptides were capable of suppressing the E2-dependent luciferase expression in the test cell line. These small peptides might be able to inhibit E2-dependent DNA replication.

Peptide therapeutics have the important advantage over small molecule drug due to the structural relationships between the constructed peptide and the physiologically active parent molecules, which reduce the risk of side reactions

(Edwards et al., 1999). In contrast, small molecules can build up in various organs, ultimately leading to severe toxic side effects. Peptide therapeutics also have disadvantages related to their *in vivo* instability such as, short half-life and low bioavailability, susceptibility to proteases. Major disadvantage of using peptides is the high production cost and the market price as compared to that of the small molecules (Craik et al., 2013).

1.9 Prevention and treatment

The first vaccines to prevent a human cancer were the vaccines that used to prevent HPV infection. Like other vaccines, they are consisted of noninfectious virus-like particles, which resemble the native virus immunologically. Two prophylactic HPV vaccines are currently licensed; bivalent vaccine and quadrivalent vaccine (Frazer et al., 2011). The bivalent vaccine incorporates two HPV types responsible for the majority of cervical cancer (HPV16 and HPV18), and a quadrivalent vaccine additionally incorporates HPV6 and HPV11 (Gnanamony et al., 2007). However, lifestyle modifications should be the first and simple way to prevent HPV and other related diseases, such as: delaying first intercourse until age 21 and limiting the number of sexual partners (Hildesheim et al., 2007). Clinical examination and screening of cellular alterations with cytology (Pap smear) on a regular basis is the next prevention step. The treatment of HPV generally involves ablative and excisional procedures that the most effective treatment of HPV and related disease, which aim to eliminate the HPV-infected cells. Ablative procedures include chemodestructive agents, like trichloroacetic acid and bichloroacetic acid, infrared coagulation, cryoablation (cryosurgery), and carbon dioxide laser ablation. Some topical treatments (5-

flurouracil, podophyllin, and podophyllotoxin), or immune-modulating therapy (topical use of imiquimod or intralesion interferon injections) can also be used (Diaz, 2008). Choice of treatment is depending on the stage of the malignancy and other factor for an advanced disease. It is common to use surgical procedures in which radiotherapy can also be included (Arbyn et al., 2012).

1.10 Objective of the dissertation

Initiation of replication of HPV DNA requires an E1-E2 complex formation. Therefore, disruption of this complex could inhibit viral propagation. In the previous study, dodecapeptides that could bind to HPV16 E2 were screened from the phage display library (Fujii et al., 2003). The peptide4 were capable of suppressing the E2-dependent luciferase expression in the tested cell line, suggesting that they might be able to inhibit E2-dependent DNA replication and could be used for controlling HPV infections. This research aim to, (i) predict the binding conformations and interactions between the peptides reported in Fujii et al 2003 and HPV16 E2, as well as to determine the key residues of peptide4 (the best binder) for E2 binding (ii) design peptide inhibitors, based on peptide4 HPV16 E2 interactions, that should be able to bind to HPV16 E2 and disrupt the E1-E2 complex formation better than peptide4 (iii) test whether the designed peptides could bind to HPV16 and disrupt the E1-E2 complex formation more effective than peptide4.

CHAPTER II

MATERIALS AND METHODS

2.1 Materials

2.1.1 Equipments

4 °C refrigerator (Sharp)

-20 °C Freezer (Whirlpool)

-80 °C Freezer (Thermo Electron Corporation)

96-well cell culture cluster, flat bottom with lid (Costar)

Autoclave model # MLS-3750 (SANYA E&E Europe (UK Branch) UK Co.)

Amicon Ultra-15 10K concentrators (Millipore)

Automatic micropipette P10, P20, P100, P200 and P1000 (Gilson Medical Electrical)

Balance PB303-s (Mettler Teledo)

Bio Clean Bench (Sanyo)

Biophotometer (Eppendorf)

Centrifuge 5804R (Eppendorf)

Gel Documentation System (GeneCam FLEX1, Syngene)

GelMate2000 (Toyobo)

Gene pulser (Bio-RAD)

Incubator 37 °C (Mettmert)

Innova 4000, 4080 incubator shaker (New Brunswick Scientific)

Kuhner LT-W incubator shaker (Lab Therm)

Microcentrifuge tube 0.6 ml and 1.5 ml (Axygen® Scientific, USA)

Microwave R362 (Sharp)

Mini Horizontal Electrophoresis System (Biolab)

Mini Personal Centrifuge micro ONE (TOMY Digital Biology)

Mini Trans-Blot Module #1703935 (Bio-RAD)

MJ Research PTC 200 PCR Thermal Cycler (Bio-RAD)

Multichannel pipette P200 (Eppendorf)

New Classic Balances (Mettler Teledo)

PCR Mastercycler (Eppendorf AG, Germany)

SevenCompact™ pH/Ion meter S220 (Mettler Teledo)

Synergy™ H1 Microplate Reader (BioTek)

Sonicator, Model VCX-500-220 (SONICS Vibracell™)

Pipette tips 10, 100 and 1000 µl (Axygen® Scientific, USA)

Power supply, Power PAC3000 (Bio-RAD Laboratories, USA)

SpectraMax M5 Multi-Mode Microplate Reader (Molecular Devices)

Thermolyne 3 Block Dri-Bath Incubator (Thermo Scientific)

Universal 320R Centrifuge (Hettich, UK)

Vortex-Genie 2 Mixer (Scientific Industries)

Water bath (Mettler)

2.1.2 Chemicals and reagents

100 mM dATP, dCTP, dGTP and dTTP (Fermentas)

2-Mercaptoethanol, C₆H₆OS (Fluka)

5-bromo-4-chloro-indolyl phosphate (BCIP) (Fermentas)

Absolute ethanol, C₂H₅OH (BDH)

Absolute methanol, CH₃OH (Scharlau)

Acetic acid glacial, CH₃COOH (BDH)

Acrylamide (Plus one)

Agarose (Sekem)

Alexa Fluor[®] 488 goat anti-rabbit IgG antibody (Invitrogen)

Alkaline phosphatase-conjugated goat anti-mouse (Millipore)

Alkaline phosphatase-conjugated goat anti-rabbit (Jackson Immuno Research Laboratories, Inc.)

Ammonium persulfate, (NH₄)₂S₂O₈ (USB)

Ampicillin (BioBasic)

Anti-biotin antibody (Abnova)

Anti-E2 monoclonal antibody (Abnova)

Anti-His antibody (GE healthcare)

Anti-MBP antibody (Abnova)

Bacto tryptone (Scharlau)

Bacto yeast extract (Scharlau)

Boric acid, BH₃O₃ (MERCK)

Bovine serum albumin (Fluka)

Bromophenol blue (MERCK)

Calcium chloride (MERCK)

Chloramphenicol (Sigma)

Coomassie brilliant blue G-250 (Fluka)

Coomassie brilliant blue R-250 (Sigma)

di-sodium hydrogen orthophosphate anhydrous, Na₂HPO₄

Ethylene diamine tetraacetic acid disodium salt dehydrate (EDTA) (Fluka)

Ethidium bromide, (Sigma)

GeneRuler™ 1 kb DNA ladder (Fermentas)

GeneRuler™ 100 bp DNA ladder (Fermentas)

Glycine, USO Grade, $\text{NH}_2\text{CH}_2\text{COOH}$ (Research organics)

Hydrochloric acid, (HCl) (Merck)

Imidazole (Fluka)

IPTG (Isopropyl- β -D-thiogalactoside), $\text{C}_9\text{H}_{18}\text{O}_5\text{S}$ (USBiological)

Kanamycin sulfate (Biobasic INC.)

Magnesium chloride, MgCl_2 (Merck)

Millipore membrane filter 0.22 and 0.45 μm (Millipore)

Ni Sepharose 6 Fast Flow (GE Healthcare)

Nitro blue tetrazolium choride, NBT (Fermentus)

Prestain protein molecular weight marker (Fermentas)

Skim milk powder (Hi-media)

Sodium acetate, CH_3COONa (Carlo Erba)

Sodium chloride, NaCl (Ajax)

Sodium dihydrogen orthophosphate, $\text{NaH}_2\text{PO}_4\text{H}_2\text{O}$ (Carbo Erba)

Sodium dodecyl sulfate (Sigma-Aldrich)

Sodium hydroxide, NaOH (Merck)

Tetramethylethylenediamine, TEMED (BDH)

Tris (Vivantis)

Triton™ X-100 (Merck)

Tween™-20 (Fluka)

Unstained protein molecular weight marker (Fermentus)

2.1.3 Enzymes

NheI, *XhoI*, *NcoI* and *EcoRI* restriction enzyme (New England Biolabs, USA)

Q5[®] High-Fidelity DNA Polymerase (New England Biolabs, USA)

T4 DNA ligase (Promega)

2.1.4 Bacterial strains

Escherichia coli strain TOP10 (Thermo Fisher Scientific)

Escherichia coli strain BL21 (DE3) (Stratagene)

2.1.5 Experiment kits

Alkaline Phosphatase Substrate Kit (Bio-RAD)

GenepHlow[™] Gel/PCR Kit (Geneaid)

pGEM[®]-T Easy Vector Systems Kite (Promega)

Presto[™] Mini Plasmid Kit (Geneaid)

2.1.6 Vectors

pET-28b(+) (Novagen)

pMAL-c5x vector (New England Biolabs)

2.1.7 Softwares

BlastX (<http://blast.ncbi.nlm.nih.gov>)

ClusPro (<https://cluspro.bu.edu/login.php>)

ClustalW2 (<http://www.ebi.ac.uk/Tools/msa/clustalw2>)

Compute pI/Mw (http://web.expasy.org/compute_pi)

GraphPad Prism Version 6.0 (GraphPad Software, San Diego, CA)

I-TASSER (<http://zhanglab.ccmb.med.umich.edu/I-TASSER>)

Swiss-PdbViewer Version 4.1 (Swiss Institute of Bioinformatics)

2.2 Prediction of HPV16 E1-E2 interactions, binding conformations and interactions between the peptides and HPV16 E2

The TAD of HPV16 E2 (residues 1-201) and the helicase domain of HPV16 E1 (residues 421-622) were used in this study. HPV16 E2 (PDB code: 2NNU, chain A) was used as a model (Abbate et al., 2004) and six amino acid residues (D25N, H35Q, T135K, H136Y, A143T and R165Q) were changed to match the sequence of HPV16 E2 protein used in *in vitro* experiments. The whole structure was minimized using Swiss-PdbViewer (Guex and Peitsch, 1997). The I-TASSER server (Roy et al., 2010, Yang et al., 2015), an on-line platform for protein structure and function predictions, was used to build the helicase domain of HPV16 E1 (residues 421-622) based on the crystal structure of HPV18 E1 (PDB code: 1TUE, chain D). Before docking calculations, the structures of E1 and E2 were assigned appropriate protonation states by PDB2PQR server (Dolinsky et al., 2004).

ClusPro, a protein-protein docking server (Comeau et al., 2004), was used in all docking simulations with default parameters “balanced coefficient” To test whether ClusPro server and its parameters could potentially be used to predict the binding conformations and interactions of the system involving E1 and E2, E1 (chain D) was redocked to E2 (chain E) of the crystal structure of HPV18 E1-E2 complex (PDB code: 1TUE). The docked conformation was reasonably similar to that of the crystal structure

of HPV18 E1-E2 complex with the value of the backbone root mean square deviation (RMSD) of 1.47 Å. After this validation, HPV16 E1 was docked to HPV16 E2, and the value of the backbone RMSD between the docked conformation and the crystal structure of HPV18 E1-E2 complex was computed.

Nine peptides (peptide1 to peptide9) reported in Fujii et al, 2003 were built by I-TASSER server. ClusPro server was used to dock these peptides to HPV16 E2, using default parameters. The centroid of the docked structures that were clustered with the highest populations was used for the analysis of the binding interactions between each peptide and E2.

2.3 Design of peptides to inhibit HPV16 E1-E2 complex

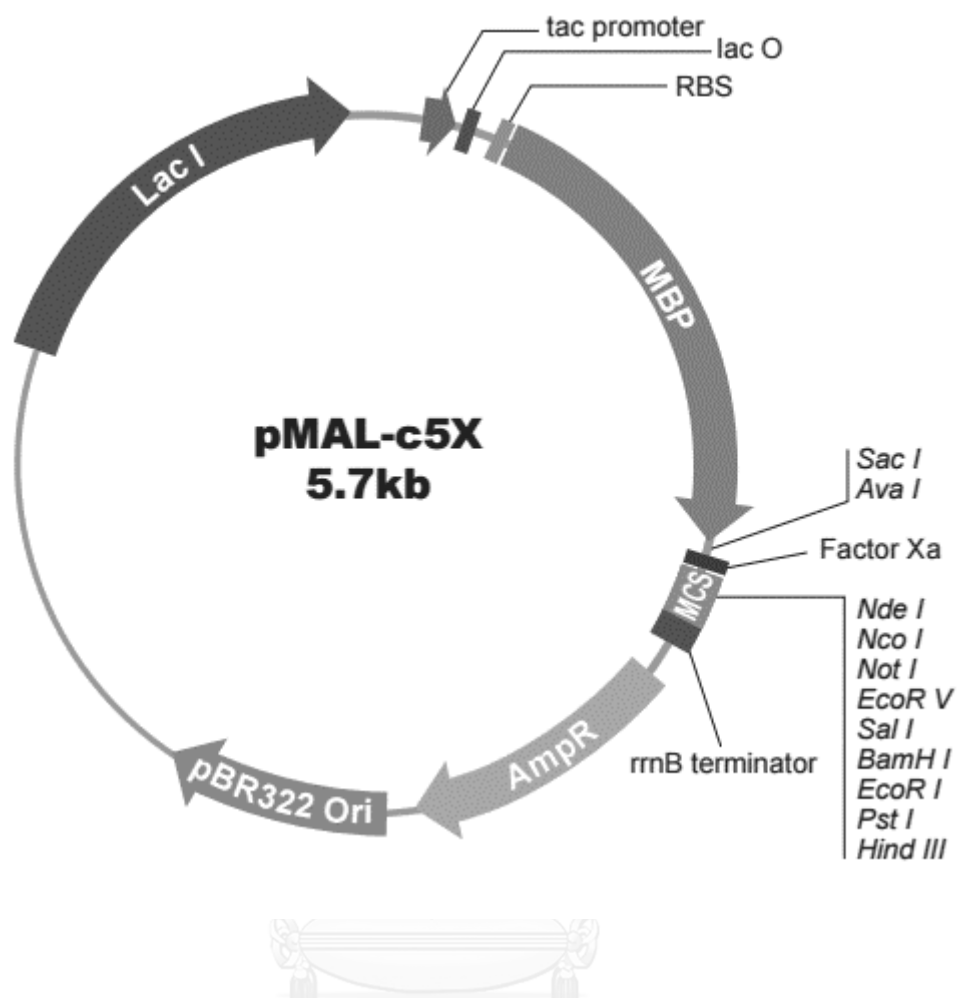
The binding conformation of peptide4 (TWFWPYPYPHLP) to HPV16 E2 was used as a design template. The structures of HPV16 E2-peptide4 and HPV16 E1-E2 complex were superimposed by Swiss-PdbViewer, and their backbone RMSD value was calculated. The amino acid positions of peptide4 within the E1-E2 complex binding interfaces were elucidated. The residues of peptide4 that should be able to favorable hydrogen bonds with HPV16 E2 and also disrupt interactions between HPV16 E1-E2 complex were proposed. The selected amino acid positions of peptide4 were mutated into 20 amino acids and rotated to all possible rotamers that could disrupt the interactions between HPV16 E1 and E2. All of the possible designed peptides were docked onto the structure of HPV16 E2 and the binding energy between each peptide and E2 protein was calculated.

2.4 Expression and purification of recombinant of HPV16 E1

2.4.1 Construction of the recombinant E1-pMAL-c5x

The nucleotides corresponding to helicase domain of HPV16 E1 (residue 421-622) were amplified by PCR using a viral HPV16 strain CU14 DNA (sequence ID: gb|JQ004098.1) as a template. The PCR product was clone into pMAL-c5x vector via *NcoI* and *EcoRI* site restriction site (Figure 8).





pMAL-c5X-His Polylinker:

5' *ma*TE...TCG AGC TCG (AAC)₄ AAT AAC AAT (AAC)₃ CTC GGG ATC GAG GGA AGG ATT TCA
 NdeI NcoI NotI EcoRV SalI BamHI EcoRI SbfI
 CAT ATG TCC ATG GGC GGC CGC GAT ATC GTC GAC GGA TCC GAA TTC CCT GCA GGT
 HindIII
 AAT CAT CAT CAT CAC CAC CAC TAA ATA AGC TT...

Figure 8 Map of pMAL-c5x

2.4.2 Primer design

The primers were designed based on nucleotides sequence of HPV16 E1 by using SECentral Program. The sequences of forward and reverse primers were shown in Table 4 The forward primer contained *NcoI* at the 5'-end and the reverse primer had *EcoRI* site restriction site and a 6xHis-tag at the 3'-end.

Table 4 List of primers used for amplification of HPV16 E1 gene (residue 421-622).

Products name	Primer	Sequence (5'-3')	T _m (°C)	GC content
HPV16 E1 (residues 421-622)	Forward (<i>NcoI</i>)	5'-CCATGGATAGTATGAG TCAATGGATAAAATATAG AT-3'	57	44%
	Reverse (<i>EcoRI</i>)	5'-GAATTCTTAGTGATGAT GATGATGATGCAAACCTTA ATCTGGACCACGTCCTT-3'	78	50%

2.4.3 PCR conditions

The fragment of HPV16 E1 gene was amplified by PCR (Table 5). The PCR condition was pre-denaturation at 98 °C for 30 seconds, and 30 cycles of denaturation at 98 °C for 10 seconds, annealing at 60 °C for 30 seconds, and extension at 72 °C for 1 minute following by final extension at 72 °C for 2 minutes. The PCR product was purified by agarose gel electrophoresis.

Table 5 PCR conditions for amplification of HPV16 E1 gene (residue 421-622).

Component	50 μ l Reaction	Final concentration
5X Q5 Reaction Buffer	10 μ l	1x
10 mM dNTPs	1 μ l	200 μ M
10 μ M Forward Primer	2.5 μ l	0.5 μ M
10 μ M Reverse Primer	2.5 μ l	0.5 μ M
HPV16 E1 gene	2	500 ng
Q5 High-Fidelity DNA Polymerase	0.5 μ l	2.5 U/ μ l
Nuclease-Free Water	To 50 μ l	-

2.4.4 Plasmid DNA extraction

The *E. coli* TOP10 harboring expression plasmid vector was grown in 5 ml Luria-Bertani (LB) broth (1% (w/v) tryptone, 1% (w/v) NaCl and 0.5% (w/v) yeast extract) containing 100 μ g/ml ampicillin at 37 °C overnight with shaking at 250 rpm. The overnight cell was collected by centrifugation at 8,000 \times g for 1 minute in 1.5 ml microcentrifuge tube. Cells were resuspended in 200 μ l of solution I (50 mM glucose, 25 mM Tris-HCl and 10 mM EDTA, pH 8.0) Then, 200 μ l of solution II (0.2 N NaOH and 1% SDS) was added, gently mixed by inverting 10 times and placed at room temperature for 5 minutes. After that, 300 μ l of solution III (3 M sodium acetate, pH 4.8) was added and gently mixed by inverting 10 times. The mixture was centrifuged at 14,000 \times g for 3 minutes and supernatant was transferred to a PDH Column. The PDH

Column was dried by centrifuge at 14,000 ×g for 30 seconds at room temperature then the flow-through was discarded. PDH Column was placed back to the microcentrifuge tube and washed with 600 µl washing buffer by centrifuge at 14,000 ×g for 30 seconds. The PDH Column was transferred to a new microcentrifuge tube and 50 µl of fresh water was added and placed at room temperature for 2 minutes. Finally, the column was centrifuged at 14,000 ×g for 2 minutes to harvest the plasmid.

2.4.5 Plasmid DNA preparation

The expression vector pMAL-c5x was linearized by restriction enzyme *NcoI* and *EcoRI*. The reaction mixture containing of 1 µg pMAL-c5x, 1x cut smart buffer (50 mM potassium acetate, 20 mM Tris-acetate, 10 mM magnesium acetate, 100 µg/ml BSA, pH 7.9), 2 U of *NcoI* and 2 U *EcoRI* in total volume of 20 µl, was incubated at 37 °C for 2 hours.

2.4.6 E1 gene fragment preparation

The amplified was digested with *NcoI* and *EcoRI*. The reaction mixture containing 1 µg E1 gene fragment, 1x cut smart buffer, 2 U of *NcoI* and 2 U *EcoRI* in total volume of 20 µl, was incubated at 37 °C for 2 hours. The DNA fragment was harvested from agarose gel by GenepHlow™ Gel/PCR Kit.

2.4.7 Purification of DNA fragments

Both digested gene and expression vector were purified by GenepHlow™ Gel/PCR Kit (Geneaid). In brief, PCR products were run on 1% agarose gel electrophoresis and digested DNA fragment products were cut from the gel and put in microcentrifuge tubes. Five hundred microliter of Gel/PCR Buffer was added to 300 mg of agarose gel and incubated at 60 °C for 15 minutes or until the gel was completely dissolved. The mixture solution was loaded onto DFH column and centrifuged at 12,000 ×g for 1 minute. The flow-through was discarded and 400 µl of W1 Buffer was added into the column. The column was centrifuged at 12,000 ×g for 1 minute and the flow-through was discarded. The DFH column was dried by centrifugation at 14,000×g for 2 minute prior to elution step. Thirty microliter of DI water was added into center of column before the column was spun at 14,000 ×g for 1 minute to harvest the DNA.

2.4.8 Determination of the quantity and quantity of DNA samples

The concentration of DNA samples could be measured by absorbance at 260 nm (A_{260}) using following formula

$$[\text{DNA}] = A_{260} \times 50 \times \text{dilution factor}$$

Absorbance at 260 nm of 1 corresponds to approximately 50 ng/µl of DNA. Absorbance at 280 nm was also measured in order to determine protein contamination. $A_{260/280}$ ratio above 1.8 indicates high purity of DNA or RNA sample.

2.4.9 Ligation of vector DNA and the E1 gene fragment

The *NcoI* and *EcoRI* digested E1 gene fragment was ligated to the *NcoI* and *EcoRI* digested pMAL-c5x vector at molar ratio of DNA vector: inserted E1 gene of 1:3. The ligation mixture of 20 μ l contained 50 ng of vector DNA, 150 ng of the gene fragment, 1x ligation buffer (50 mM Tris-HCl, pH 7.6, 10 mM MgCl₂, 1 mM ATP, 1 mM DTT and 5% (W/V) polyethylene glycol) and 1 U of T4 DNA ligase. The ligation mixture was incubated at room temperature for 1 hour. The reaction mixture 2 μ l was then transformed into *E. coli* TOP10.

2.4.10 *E. coli* competent cell preparation

A single colony of *E. coli* was inoculated into LB broth and incubated with 250 rpm shaking at 37 °C overnight. Overnight cultured of *E. coli* was inoculated into a fresh 100 ml LB broth in 1:100 dilution and incubated with continuous shaking at 37 °C until the absorbance at 600 nm (OD₆₀₀) reach 0.3-0.4. Cells were chilled on ice for 20 minutes and centrifuged at 2,000 \times g for 10 minutes at 4 °C. Cell pellet was gently resuspended in 20 ml of pre-cool 100 mM CaCl₂ solution and centrifuged at 2,000 \times g for 20 minutes at 4 °C. Cell pellet was then resuspended in 4 ml of chilled 10 mM CaCl₂ solution and dispensed as 100 μ l aliquots and stored at -80 °C until use.

2.4.11 Transformation

The recombinant plasmids were transformed into competent cell of *E. coli* BL21 (DE3) by heat shock. The competent cell was placed on ice for 5 minutes. The recombinant plasmids (5ng) was added into competent cell and incubated on ice for 20 minutes. The mixture was then heated at 42 °C for 45 seconds and incubated on ice for 2 minutes to reduce damage to the *E.coli* cells. LB broth of 1 ml (with no antibiotic) was added and cells were incubated for 1 hour at 37 °C with shaking at 200 rpm. Cells were spread onto LB agar plates containing antibiotic (30 µg/ml of kanamycin for E2-pET28 or 100 µg/ml of ampicillin for E1-pMAL-c5x) and incubated at 37 °C for 16 hours. *E. coli* containing the recombinant plasmid which could grow on an antibiotic plate was picked and the plasmid was isolated.

2.4.12 Expression of HPV16 E1 gene

E. coli strain BL21 (DE3) harboring E1 recombinant plasmid were grown in LB broth containing 0.1 mg/ml ampicillin and 0.2% glucose at 37 °C overnight. The overnight cultures were inoculated into fresh LB and grew until OD₆₀₀ reached 0.5. A final concentration of 0.3 M isopropyl-β-D-thio-galactoside (IPTG) was added into *E. coli* culture. Cells were grown for 2 hours at 37°C at 250 rpm and then harvested. The *E. coli* culture was sonicated (microtip 21%, pulse-on 1 second, pulse-off 1 second of 20 minutes) and the supernatant and pellet were separated by centrifugation. Sodium dodecyl polyacrylamide gel electrophoresis (12% SDS-PAGE) and Western blot were used to analyze the supernatant and pellet fractions. Anti-MBP antibody (Abnova) was used to probe the (MBP)-tagged fusion E1.

2.4.13 Purification of recombinant HPV16 E1

E. coli strain BL21 (DE3) harboring E1 recombinant plasmid were expressed as described in 2.4.12. The cells were resuspended in 1x PBS buffer, pH 7.4 (PBS; 137 mM NaCl, 2.7 mM KCl, 10 mM Na₂HPO₄, 2 mM KH₂PO₄) and sonicated (microtip 21%, pulse-on 1 second, pulse-off 1 second of 20 minutes). The lysate was clarified by centrifugation at 8,000 ×g, 4 °C for 30 minutes and then loaded onto a Ni Sepharose™ 6 Fast Flow column (GE Healthcare) equilibrated in 1x PBS and 20 mM imidazole. After washing, the protein was eluted from the column with 1x PBS containing 500 mM imidazole. Protein fractions were then analyzed by 12% SDS–PAGE. Bicinchoninic acid (BCA) protein assay (Pierce) was used to determine the concentration of purified protein. Western blotting was performed to detect the MBP (Maltose binding protein)-tagged fusion E1 using a primary anti-MBP antibody (Abnova).

2.5 Expression and purification of recombinant of HPV16 E2

2.5.1 Construction of the recombinant of E2-pET28b(+)

The nucleotide encoding the transactivation domain (residues 1-201) of E2 was cloned into pET28b(+) vector (Figure 9). The viral HPV16 strain CU14 DNA (sequence ID: gb|JQ004098.1|) was used as a template for amplification of the truncated E2 gene.

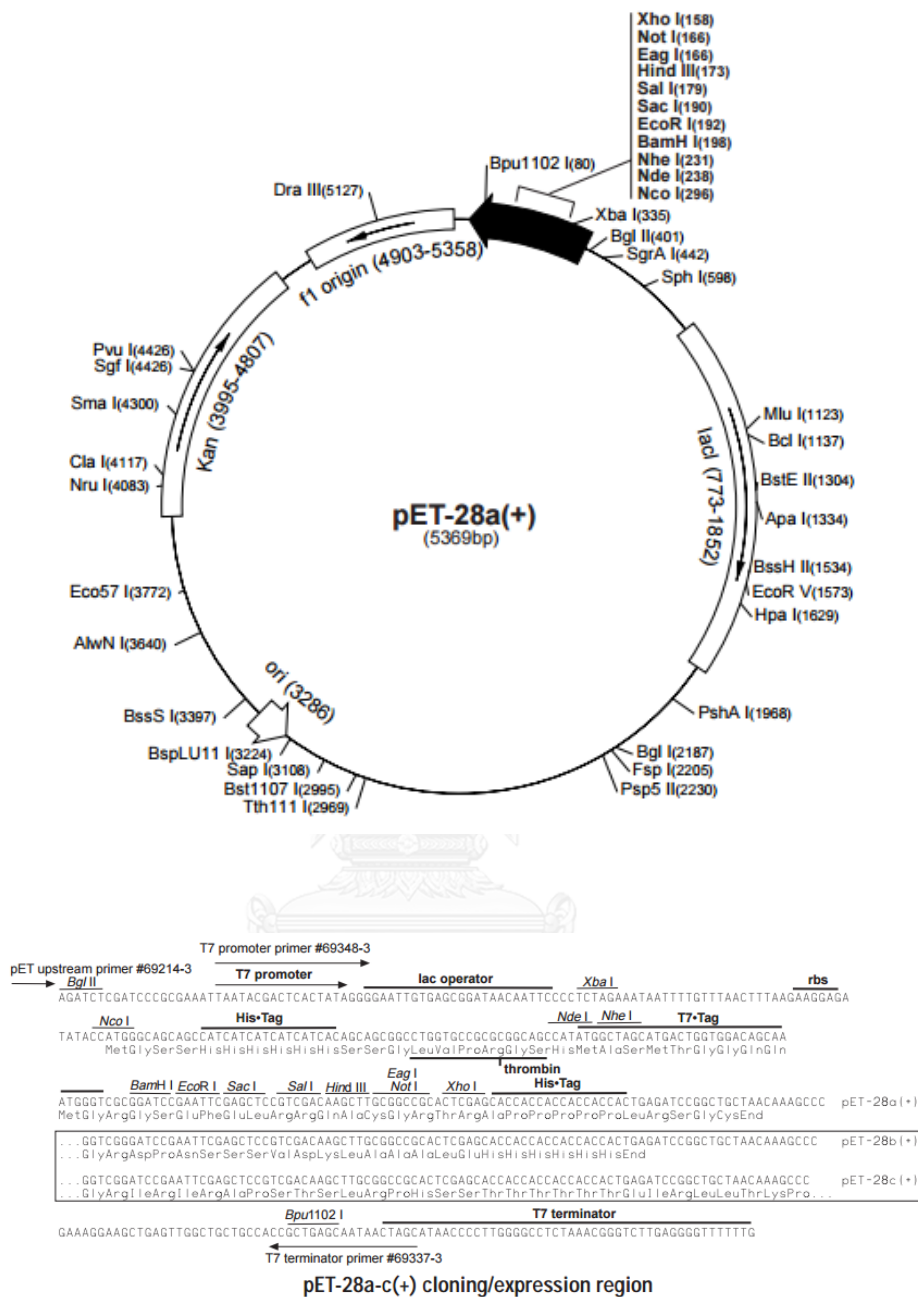


Figure 9 Map of pET28b(+)

2.5.2 Primer design

The primers were designed based on nucleotides sequence of HPV16 E2 using SECentral Program. *NheI* restriction site and 6xHis-Tag were introduced at the 5'-end of the forward primer. *XhoI* restriction site was added at the 3'-end of the reverse primer. The sequences of forward and reverse primers were shown in Table 6.

Table 6 List of primers used for amplification of truncated HPV16 E2 gene (residues 1-201).

Products name	Primer	Sequence (5'-3')	T _m (°C)	GC content
HPV16 E2 (residues 1-201)	Forward (<i>NheI</i>)	5'-AGCTAGCATGGAGA CTCTTTGCCAACG-3'	74	51.8%
	Reverse (<i>XhoI</i>)	5'-CCTCGAGCTAGCTAAA CACAGATGTAGGACATAA TATTAC-3'	60	40%

2.5.3 PCR conditions

The fragment of HPV16 E2 gene was amplified by PCR (Table 7). The PCR condition was pre-denaturation at 98 °C for 30 seconds, and 30 cycles of denaturation at 98 °C for 10 seconds, annealing at 66 °C for 30 seconds, and extension at 72 °C for 1 minute, followed by final extension at 72 °C for 2 minutes. The PCR product was purified by agarose gel electrophoresis.

Table 7 PCR conditions for amplification of HPV16 E2 gene (residues 1-201).

Component	50 μ l Reaction	Final concentration
5X Q5 Reaction Buffer	10 μ l	1x
10 mM dNTPs	1 μ l	200 μ M
10 μ M Forward Primer	2.5 μ l	0.5 μ M
10 μ M Reverse Primer	2.5 μ l	0.5 μ M
HPV16 E2 gene	2	500 ng
Q5 High-Fidelity DNA Polymerase	0.5 μ l	2.5 U/ μ l
Nuclease-Free Water	To 50 μ l	-

2.5.4 Plasmid DNA preparation

The expression vector pET28b(+) vector was linearized by restriction enzyme *Nhe* I and *Xho*I. The reaction mixture containing 1 μ g pET28b vector, 1x cut smart buffer 2 U of *Nhe* I and 2 U *Xho*I in total volume of 20 μ l, was incubated at 37 °C for 2 hours.

2.5.5 E2 gene fragment preparation

The PCR product from 2.5.3 was digested with *Nhe*I and *Xho*I. The reaction mixture containing 1 μ g E2 gene fragment, 1x cut smart buffer, 2 U of *Nhe*I and 2 U *Xho*I in total volume of 20 μ l, was incubated at 37 °C for 2 hours. The DNA fragment was harvested from agarose gel by GenepHlow™ Gel/PCR Kit.

2.5.6 Ligation of vector DNA and the E2 gene fragment

The *Nhe* I and *Xho*I digested E2 gene fragment was ligated to the *Nhe*I and *Xho*I digested pET28b(+) vector at molar ratio of DNA vector: inserted E2 gene of 1:3. The ligation mixture of 20 μ l contained 50 ng of vector DNA, 150 ng of the gene fragment, 1x ligation buffer and 1 U of T4 DNA ligase. The ligation mixture was incubated at room temperature at 1 hour. The reaction mixture was then transformed into *E.coli* TOP10.

2.5.7 Expression of HPV16 E2 gene

Recombinant E2-pET28 was expressed in *E. coli* strain BL21 (DE3). The single colony of *E. coli* harboring recombinant plasmid was grown in LB broth containing 15 μ g/ml kanamycin at 37 °C overnight. The overnight cultures were grown in fresh LB until OD₆₀₀ reached 1.2 then induced with a final concentration of IPTG of 0.3 mM. The cells were incubated for 16 hours at 16°C with 250 rpm shaking and harvested by centrifugation at 8,000 \times g for 30 min. The cells were sonicated (microtip 21%, pulse-on 1 second, pulse-off 1 second of 20 minutes) and centrifuged at 8,000 \times g for 30 minutes to separate the supernatant. 12% SDS-PAGE was used to analyze the supernatant and pellet fractions.

2.5.8 Purification of recombinant HPV16 E2

E. coli strain BL21 (DE3) harboring E2 recombinant plasmid were expressed as described in 2.5.7. Cells were resuspended in 1x PBS buffer, pH 7.4 (PBS; 137 mM NaCl, 2.7 mM KCl, 10 mM Na₂HPO₄, 2 mM KH₂PO₄) and sonicated (microtip 21%, pulse-on 1 second, pulse-off 1 second of 20 minutes). The lysate was clarified by

centrifugation at 8,000 \times g, 4 °C for 30 minutes and then loaded onto a Ni Sepharose™ 6 Fast Flow column (GE Healthcare) equilibrated in 1x PBS and 20 mM imidazole. After washing, the protein was eluted from the column with 1x PBS containing 500 mM imidazole. Protein fractions were then analyzed by 12% SDS–PAGE. Bicinchoninic acid (BCA) protein assay (Pierce) was used to determine the concentration of purified protein. Western blotting was performed to detect the His-tagged fusion E2 using a primary mouse anti-E2 antibody (Abnova) in PBS/Tween20 containing 1% (w/v) skim milk. The secondary antibody is anti-mouse IgG conjugated alkaline phosphatase (AP) that specific to anti-E2 antibody in 1% (w/v) skim milk in PBS/Tween20.

2.6 Protein analysis

2.6.1 SDS–PAGE

The purity of protein was analyzed by SDS-PAGE. 5X SDS loading dye (60 mM Tris-HCl, pH 6.8, 25% glycerol, 2% SDS, 0.1% bromophenol blue, and 14.4 mM 2-mercaptoethanol) was mixed with proteins and boiled for 10 minutes. Both separating and stacking gel were prepared (Appendix). A protein molecular weight marker and protein samples were loaded into each well. Electrophoresis was performed using 1X SDS running buffer (25 mM Tris-HCl, pH 8.3, 192 mM glycine, and 0.1% (w/v) SDS) at a constant 25 mA per gel. The gel was then stained by coomassie blue staining solution for 1 hour. The gel was then destained in 10% (v/v) methanol and 10% (v/v) glacial acetic acid solution until the protein bands clearly appeared on the gel.

2.6.2 Western blot analysis

The SDS-PAGE gel was soaked with transfer buffer (25 mM Tris base, 150 mM glycine and 20% methanol) for 30 minutes. The supporting paper was placed onto Mini Trans-Blot Module (Bio-RAD) platform, followed by nitrocellulose membrane, SDS-PAGE gel, and the supporting paper. Protein transfer was run at a constant 350 mA for 30 minutes. The nitrocellulose membrane was soaked in blocking solution (5% (w/v) skim milk in PBS and 0.05% (v/v) Tween™-20 (PBS/Tween20) at least 3 hours at room temperature. The membrane was washed 3 times for 10 minutes with PBS/Tween20. After washing the 1:5,000 primary antibody in PBS/Tween20 containing 1% (w/v) skim milk was added and incubated for 1 hour at 37 °C. After incubation, membrane was washed 3 times for 10 minutes with PBS/Tween20 and incubated with 1:10,000 secondary antibody conjugated alkaline phosphatase (AP) in 1% (w/v) skim milk in PBS/Tween20 for 1 hour at room temperature. Membrane was washed 3 times and placed into detection buffer (100mM Tris-HCl, pH 9.5, 100 mM NaCl, 50 mM MgCl₂, 375 µg/ml NBT and 188 µg/ml BCIP) until protein bands were detected.

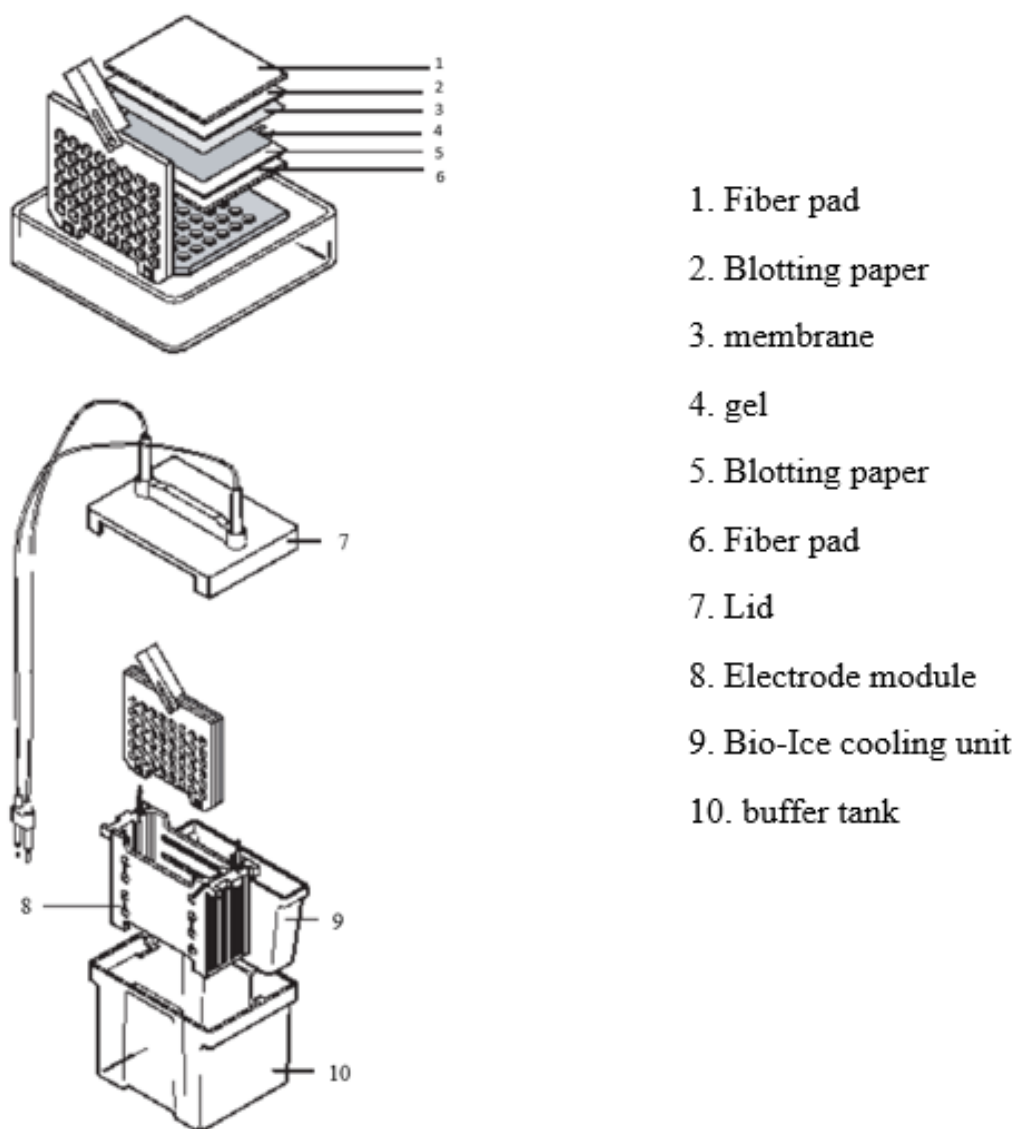


Figure 10 Exploded view of the Trans-Blot Module (Bio-RAD)

(Source: http://www.bio-rad.com/webroot/web/pdf/lsc/literature/Bulletin_5478A.pdf)

2.7 Binding assays

2.7.1 Binding of HPV16 E1 and E2

Quantitative binding assay of purified recombinant HPV16 E1 and E2 from *E. coli* were performed by an enzyme-linked immunosorbent assay (ELISA). A microtiter plate was coated with 100 μ l of HPV16 E2 (30 μ g/ml) and the excess E2 was washed out with wash buffer (PBS containing 0.05% (v/v) TweenTM-20 twice). The plate was then blocked with 1% (w/v) BSA in PBS and washed with wash buffer twice. A hundred microliter of various concentrates of HPV16 E1 was added and incubated at 25 °C for 2 h. The plate was washed with PBS twice before adding 100 μ l of anti-MBP antibody in PBS 1:5,000 (v/v) and incubate at 25 °C for 2 h. After washing, the plate was incubated with 100 μ l of alkaline phosphatase-conjugate secondary antibody against IgG (Abnova) in PBS 1:10,000 (v/v), at 25 °C for 2 h. Next, the plate was washed with wash buffer, followed by addition of 100 μ l of substrate solution (*p*-nitrophenyl phosphate) and incubation for 15 min. The reaction was measured at A₄₀₅ by SynergyTM H1 Microplate Reader (BioTek). The dissociation constants (K_d) parameter was calculated with GraphPad Prism Version 6.0 (GraphPad Software, San Diego, CA), using nonlinearly fitting as one site – Specific binding with Hill slope equation

$$Y = (B_{\max} \cdot [X]^h) / ((K_d)^h + [X]^h) \quad (\text{Eq.1})$$

where Y is the recorded absorbance, B_{\max} is the maximum specific binding (absorbance), $[X]$ is the protein concentration, h is the Hill slope and K_d is the apparent dissociation constant.

To confirm immobilized E2 has no effect on E1-E2 binding, a microtiter plate was coated with E1 and titrated with various concentrations of E2. The anti-E2

monoclonal antibody (Abnova) was used to detect E2 and the K_d values calculated from two different approaches were compared. In addition, to confirm that the MBP tag on E1 protein has not effect on E1-E2 binding, a microtiter plate was coated with E2 and titrated with increasing amounts of MBP. The anti-MBP (Abnova) was used to detect MBP and the K_d value was calculated. The experiment was carried out in triplicates.

2.7.2 Binding of designed peptides to HPV16 E2

A microtiter plate was coated with E2, followed by addition of various concentrations of peptides (0-10 μ M), which were conjugated with biotin. The anti-biotin antibody (Abnova) was used to probe E2-peptide binding. The K_d value of E2-peptide complex was calculated using Eq. 1. The experiment was carried out in triplicates.

2.7.3 Determination of the inhibitory concentration 50% (IC₅₀) of designed peptides that disrupt E1-E2 binding

A microtiter plate was coated with E2, and then washed and added various concentrations of designed peptides. After washed off excess peptides, 100 μ l of HPV E1 (1 μ M) was added and incubated at 25 °C for 2 h. The plate was then washed and incubated with 100 μ l of anti-MBP in PBS 1:5,000 (v/v). After 2 h incubation, the plate was washed and incubated with alkaline phosphatase-conjugate secondary antibody against IgG at 1:10,000 dilution. A hundred microliter of *p*-nitrophenyl phosphate was then added and incubated for 15 min. The recorded A_{405} was plotted against the peptide concentration and the data were fitted to the nonlinearly fitting as log(agonist) vs response (three parameters).

$$Y = \text{Bottom} + (\text{Top}-\text{Bottom})/(1+10^{-(X-\text{LogIC}_{50})}) \quad (\text{Eq.2})$$

Where Y is the recorded absorbance, Top and Bottom are plateaus in the units of the Y axis, X is the peptide concentration and IC_{50} is the log of the concentration of peptide that results in binding halfway between Bottom and Top. The experiment was carried out in triplicates.



CHAPTER III

RESULTS

3.1 Structural similarity between HPV16 and HPV18 E1-E2 complexes

Model of HPV16 E2 (residues 1-201) was re-built using crystal structure PDB code: 2NNU chain A as a template. Six amino acid residues (D25N, H35Q, T135K, H136Y, A143T and R165Q) were changed from the template molecule to match the sequence of HPV16 E2 used in *in vitro* experiments. The helicase domain of HPV16 E1 (residues 421-622) was built by I-TASSER server. Both HPV16 E1 and E2 structure were superimposed to crystal structure of HPV18 E1 and E2 (PDB code: 1TUE chain D and 2NNU chain A, respectively). The structures of superimposition showed high structural similarity as their calculated RMSD were quite low (1.39 Å of E1 and 1.31 Å of E2 show in Figure 11 A and B). The predicted structure of HPV16 E1 and E2 were docked with ClusPro and the docked conformation was re-docked to the crystal structure of HPV18 E1-E2 complex (PDB code: 1TUE). The structures of superimposition of HPV16 E1-E2 and HPV18 E1-E2 complex have high structural similarity (RMSD = 1.11 Å, shown in Figure 11C).

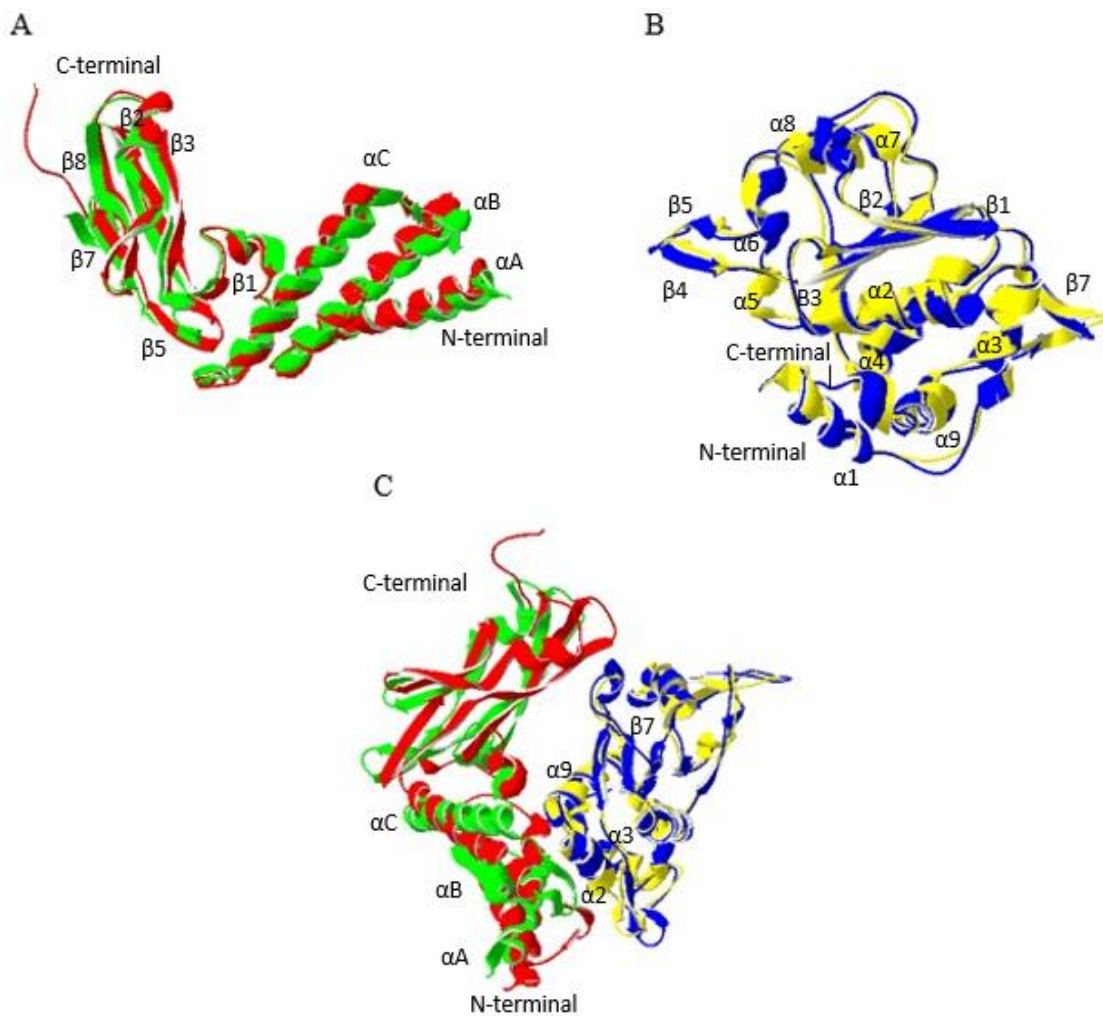
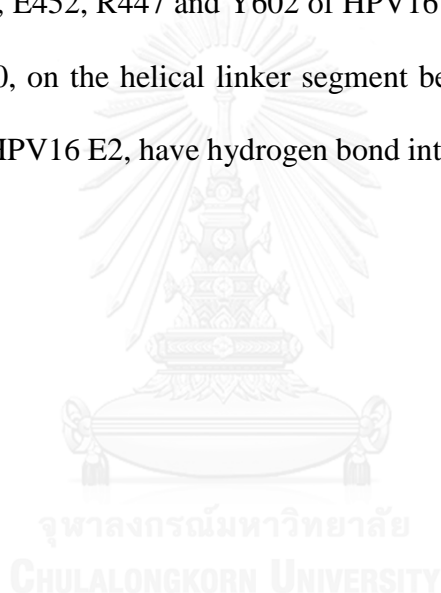


Figure 11 Superimposition of the predicted HPV16 E1-E2 and HPV18 E1-E2 complexes. (A) Superimposition of the structures of HPV16 E2 (red) and HPV18 E2 (green), RMSD = 1.31 Å. (B) Superimposition of the predicted structure of HPV16 E1 (yellow) and the crystal structure of HPV18 E1 (blue), RMSD = 1.39 Å. (C) Superimposition of the predicted structure of HPV16 E1-E2 and the crystal structure of HPV18 E1-E2 complexes RMSD = 1.11 Å.

3.2 Analysis of HPV16 E1-E2 interactions

Hydrogen bonds within HPV16 E1-E2 interaction surface were determined by Swiss-PdbViewer. Three interacting sites were observed in E1-E2 complex, including at (1) E118, N127, M129, Y178 on β 3-strand domain of HPV16 E2 forming hydrogen bonds with Y578, R575, S574, D573 of HPV16 E1, respectively (Figure 12B). (2) The N-terminal helical domain of HPV16 E2 is the major contact site for HPV16 E1, where D13, T17, Y19, D22, Y32, E39 and V58 of HPV16 E2 interact with R615 (to D13 and T17 E2), R447, R619, E452, R447 and Y602 of HPV16 E1, respectively (Figure 12D, C). (3) Q95 and E100, on the helical linker segment between the N-terminal and C-terminal domains of HPV16 E2, have hydrogen bond interactions with R462 and S455 of HPV16 E1.



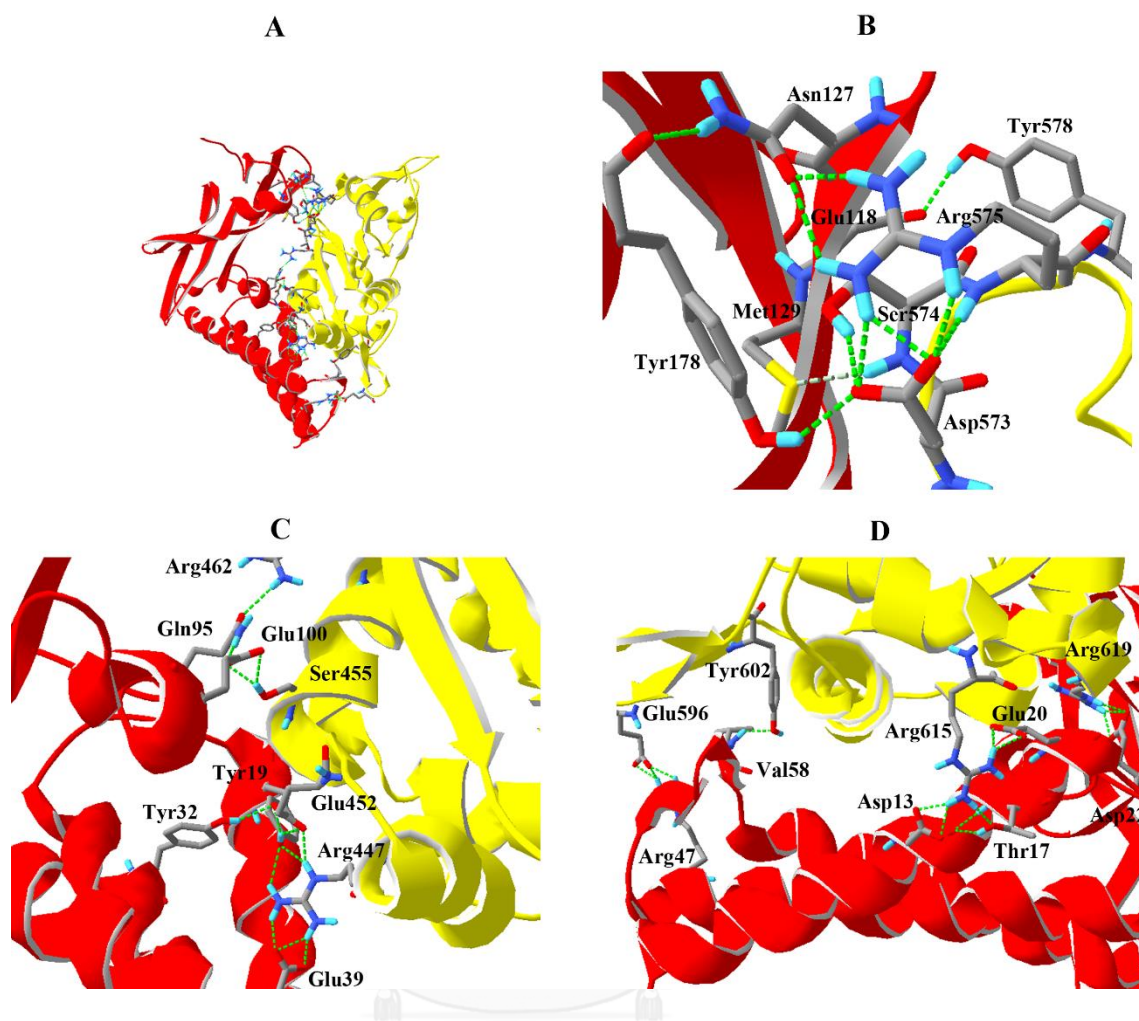


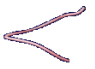





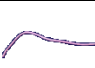

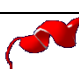
Figure 12 Analysis of HPV16 E1-E2 interactions. (A) Structure of the predicted HPV16 E1-E2 complex. The amino acid residues in the interface of E1 (yellow) and E2 (red) are labeled as grey (carbon), blue (nitrogen) and red (oxygen). Hydrogen bonds are represented by green dashed lines. Interactions between the β 3-strand domain of E2 and long loop region between β 7 and α 9 of E1 are shown in (B), while contact positions of the linker segment and the N-terminal helical domain of E2 and E1 are shown in (C) and (D).

3.3 Construction of the peptides structures using I-TASSER

Nine peptides reported in Fujii et al, 2003 were built by I-TASSER server and docked into HPV16 E2 structure by ClusPro using default parameters. Table 8 shows the best structures and the C-scores of the nine peptides. The constructed structures had reasonable topological accuracies as their C-scores were more than -1.5 (Roy et al., 2010). All of these peptides with structures shown in Table 8 were employed in the docking calculations to HPV16 E2. The trend of the lowest binding energies of the largest clusters (the best binding conformations) of each peptide was reasonably correlated with the trend of the experimental A values in Fujii et al, 2003 (Table 9).

Table 9 shows docking results between HPV16 E2 and the nine peptides. The values of the lowest binding energy of each peptide were correlated with the experimental A values, which indicated binding affinity of the peptides to E2 (low binding energy and high of A value indicate that the peptide binds to E2 with high affinity). Only peptide 1-6 and peptide9 were found within the E1-E2 binding interface, while peptide 7 and 8 were predicted to bind outside E1-E2 binding interface (Figure 13). Among nine peptides, peptide4 is the best binder to E2 since it has the lowest binding energy (-713.6 kcal/mol) (Table 9).

Table 8 The best structures and the C-scores of the nine peptides constructed by I-TASSER.

Peptide	Amino acid sequence	C-score	Structure
peptide1	TFWWHPNYYVDW	-0.66	
peptide2	TLWPWAWRHNWQ	-0.66	
peptide3	TWFNPFGYYSWA	-0.97	
peptide4	TWFWPYPYPHLP	-0.77	
peptide5	TWWTGTYPWYPR	-1.14	
peptide6	ENGLHNRSLNPR	-1.38	
peptide7	GQPSHDPVPPTT	-1.02	
peptide8	SSTSTVTPAHST	-1.21	
peptide9	SSPLAHYLNAPT	0.15	

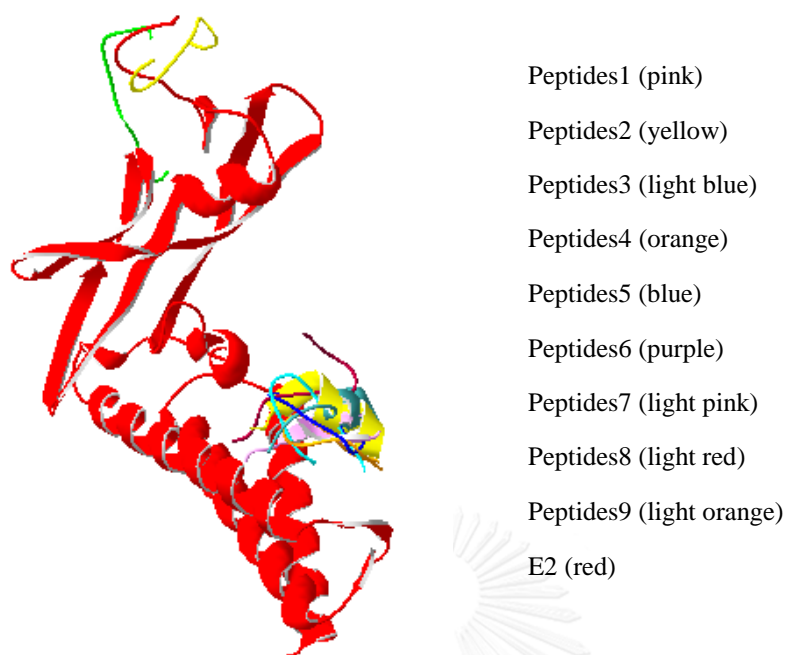


Figure 13 Docking of HPV16 E2 and nine peptides. Only peptide 1-6 and peptide9 were found within major contact region of E1 and E2, while peptide7 and 8 were predicted to bind outside E1-E2 interface.

Table 9 The lowest binding energies of the largest clusters (the best binding conformations) of the peptides to HPV16 E2, compared to their experimental A values.

Peptide	Amino acid sequence	Lowest Energy (kcal/mol)	A value*	Location of peptide within the E1-E2 binding interface
Peptide1	TFWWHPNYYVDW	-705.8	0.15	YES
Peptide2	TLWPWAWRHNWQ	-708.4	0.43	YES
Peptide3	TWFNPFGYYSWA	-694.0	0.49	YES
Peptide4	TWFWPYYPHLP	-713.6	0.53	YES
Peptide5	TWWTGTYPWYPR	-712.6	0.48	YES
Peptide6	ENGLHNRSLNPR	-519.4	0.05	YES
Peptide7	GQPSHDPVPPTT	-570.9	0.05	NO
Peptide8	SSTSTVTPAHST	-539.6	0.06	NO
Peptide9	SSPLAHYLNAPT	-502.3	0.08	YES

* A value is the absorbance value of the binding of isolated phage clones containing random peptides to the HPV 16 E2 protein by ELISA, High A-value indicates high binding affinity to E2.

3.4 Design of peptides to inhibit HPV16 E1-E2 complex

Peptide4 (the best binder to HPV16 E2) was used to design peptide inhibitor. The structures of HPV16 E2-peptide4 and HPV16 E1-E2 complex were superimposed by Swiss-PdbViewer. Figure 14 showed binding conformation and interactions of peptide4 (TWFWPYPYPHLP) with hydrogen bond. TYR6 and TYR8 of peptide4 were predicted to have hydrogen bond with HPV16 E2. TYR6 of peptide4 formed a hydrogen bond with M36 of E2 and TYR8 form hydrogen bonds with E12, E39 of E2 as well as van der Waals interactions at nearby residues. To design a small peptide inhibitor, other amino acid residues of peptide4 were mutated to 20 amino acids and rotated to all possible rotamers. TRP2, TRP4, TYR6, TYR8 and LEU11 of peptide4 could potentially form favorable hydrogen bonds with HPV16 E2. In these five residues, only two residues, TRP4 and TYR6 could potentially obstruct the binding interactions between HPV16 E1 and E2. TRP4 was mutated to His, Asn and Ser (His and Asn could potentially form a hydrogen bond with E39 of E2; Ser could potentially form a hydrogen bond with R19 of E2) (Figure 15). TYR6 was mutated to Lys, Asn and Arg (Lys could potentially form a hydrogen bond with Y19 of E2; Asn could potentially form a hydrogen bond with Y32 of E2; Arg could potentially form a hydrogen bond with E100 of E2) (Figure 16). All of these mutated peptides were then constructed by I-TASSER server and docked to HPV16 E2 structure by ClusPro server. Only five peptides (W4H, W4H_Y6K, W4H_Y6R, W4N_Y6R and Y6R) showed the lowest binding energies of the largest clusters lower than that of peptide4 and located within E1-E2 interface (Table 10 and Figure 17). These peptides are subjected to *in vitro* experiments.

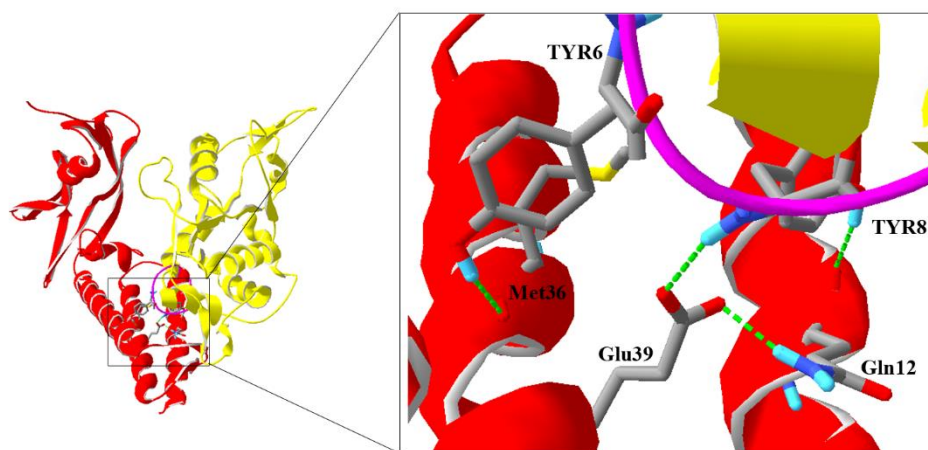


Figure 14 Binding conformation and interactions of peptide4, the best E2 binder, within HPV16 E1-E2 interface. TYR6 and TYR8 of peptide4 (TWFWPYPYPHLP) form hydrogen bonds (green dash line) with HPV16 E2 (red). HPV16 E1 and E2 displays in yellow and red, respectively. Carbons, nitrogens and oxygens are grey, blue, red, respectively.

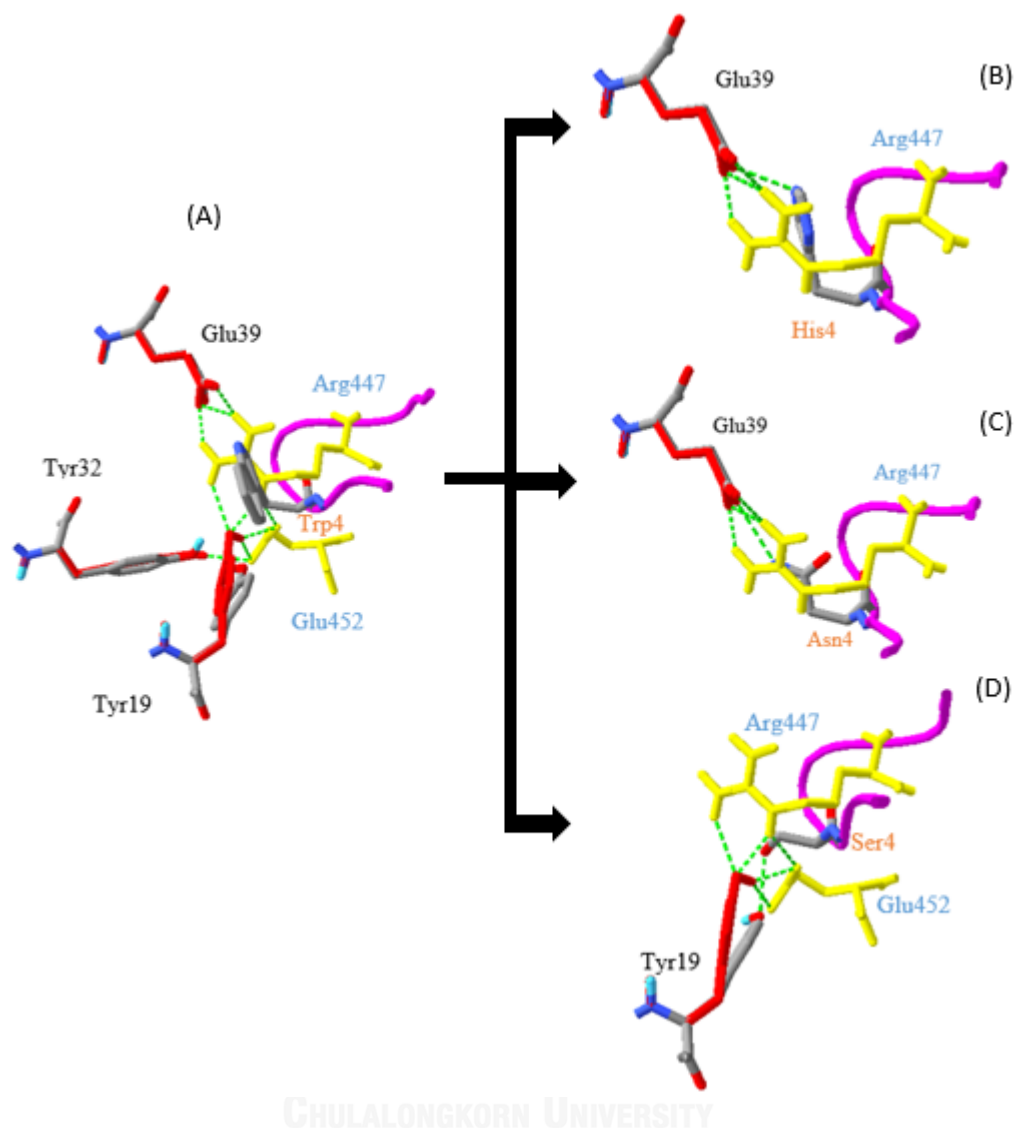


Figure 15 Design of peptides to disrupt interactions between HPV16 E1 and E2 by mutating TRP4 of peptide4. (A) position of TRP4 of peptide4 within E1 and E2 interface. TRP4 of peptide4 was mutated to His (B), Asn (C) and Ser (D). Amino acid residues in E1, E2 and peptide4 are displayed in yellow, red and pink, respectively. Mutated amino acids of peptide4 are shown in grey.

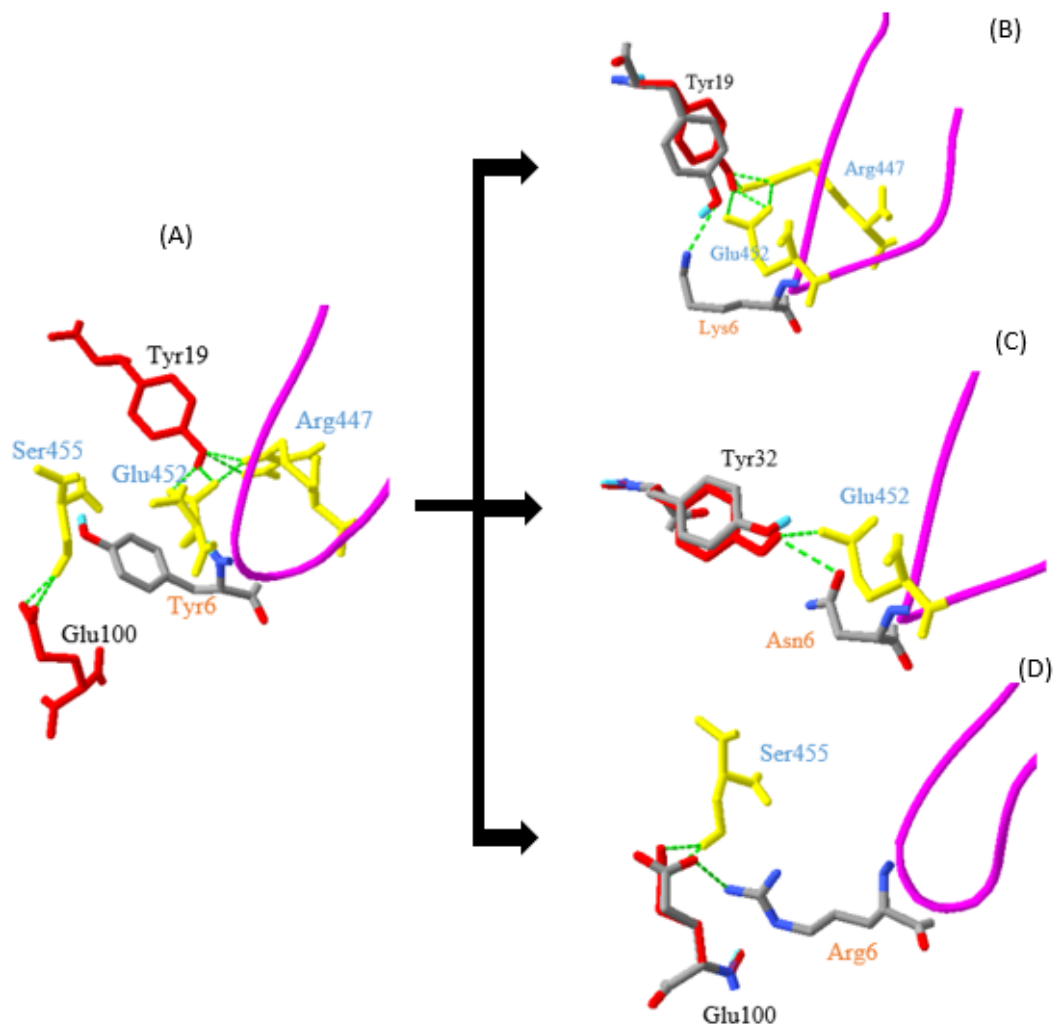








Figure 16 Design of peptides to disrupt interactions between HPV16 E1 and E2 by mutating TYR6 of peptide4 to Lys, Asn and Arg. (A) position of TYR6 of peptide4 within E1 and E2 interface. TYR6 of peptide4 was mutated to Lys (B), Asn (C) and Arg (D). Amino acid residues in E1, E2 and peptide6 are displayed in yellow, red and pink, respectively. Mutated amino acids of peptide6 are shown in grey.

Table 10 The lowest binding energies of the largest clusters of the designed peptides inhibitors targeting HPV16 E2.

Peptide	Amino acid sequence	Binding Energy (kcal/mol)	Structure
Peptide4	TWFWPYYPYPHLP	-713.6	
W4H	TWFHPYYPYPHLP	-777	
W4H_Y6K	TWFHPKPYYPYPHLP	-739.1	
W4H_Y6R	TWFHPRPYYPYPHLP	-791.1	
W4N_Y6R	TWFNPRPYYPYPHLP	-744.5	
Y6R	TWFWPRPYYPYPHLP	-830.8	

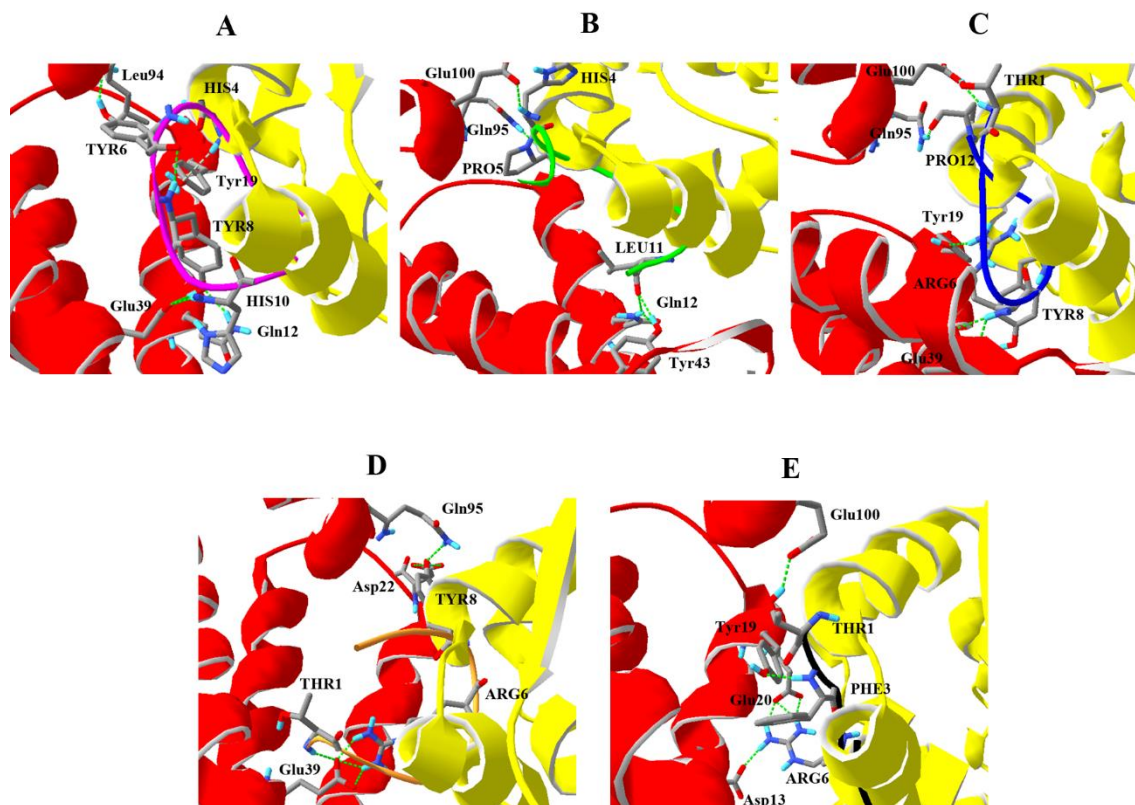


Figure 17 Binding conformations and interactions of designed peptides within HPV16 E1-E2 interface. HPV16 E1 and E2 are displayed in yellow and red, respectively. (A) W4H (TWFHPYPYPHLP) (pink). (B) W4H_Y6K (TWFHPKPYPHLP) (green). (C) W4H_Y6R (TWFHPRYPYPHLP) (blue) (D) W4N_Y6R (TWFNPRYPYPHLP) (orange) and (E) Y6R (TFWPRYPYPHLP) (black).

3.5 Cloning, expression and purification of HPV16 E1

3.5.1 Construction of E1-pMAL-c5x

Recombinant E1-pMAL-c5x plasmid was constructed in order to express HPV E1 protein in soluble form. A DNA fragment of HPV16 E1 gene (helicase domain of HPV16 E1, residue 421-622) was amplified by PCR using a viral HPV16 strain CU14 DNA (sequence ID: gb|JQ004098.1|) as a template. The PCR product was cloned into pMAL-c5x vector via *Nco* I and *Eco*RI restriction sites. The recombinant E1-pMAL-c5x was digested by *Nco*I-*Eco*RI and analyzed by agarose gel electrophoresis. Figure 18 showed that recombinant E1-pMAL-c5x plasmid contained an insert DNA fragment of approximately 600 bp, which is the expected size of truncated E1 gene. The recombinant E1-pMAL-c5x was sequenced and blasted by blastX program. The blastX showed that recombinant E1-pMAL-c5x plasmid has highest similarity to helicase domain of HPV16 E1 with 100% identity (Figure 19).

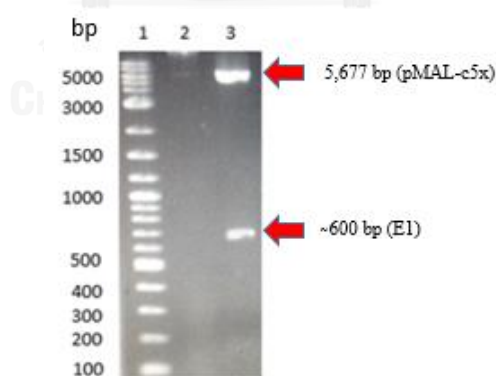


Figure 18 Analysis of recombinant E1-pMAL-c5x plasmid by *Nco*I- *Eco*RI digestion

Lane 1 : 100 bp plus DNA ladder (Fermentus)

Lane 2 : pMAL-c5x after *Nco*I and *Eco*RI digestion

Lane 3 : Recombinant E1-pMAL-c5x after *Nco*I and *Eco*RI digestion

```

HPV16          1 ----- 0
ABA86972       1 MADPAGTNGEEGTGCNGWFYVEAVVEKKTGDAISDDENENDSOTGEDLVD 50
HPV16          1 ----- 0
ABA86972       51 FIVNDNDYLTQAETETAHALFTAQEAQHRDAVQVLKRKYLGSPLSDISG 100
HPV16          1 ----- 0
ABA86972      101 CVDNNISPRLKAICIEKQSRRAAKRRLFESEDSGYGNTVEVETQQMLQVEGR 150
HPV16          1 ----- 0
ABA86972      151 HETETPCSQYSGGSGGGCSQYSSGSGGEGVSRHTICQTPLTNILNWLKT 200
HPV16          1 ----- 0
ABA86972      201 SNAKAAMLAKFKELYGVVSFSELVRPFKSNKSTCCDWCIAAFGLTPSIADS 250
HPV16          1 ----- 0
ABA86972      251 IKTLLQQYCLYLHIQSLACSWGMMVLLLVRYKCGKNRETIEKLLSKLLCV 300
HPV16          1 ----- 0
ABA86972      301 SPMCMHIEPPKLRSTAAALYWYKTGISNISEVYGDTPEWIQRQTVLQHSF 350
HPV16          1 ----- 0
ABA86972      351 NDCTFELSQMVMQWAYDNDIVDDSEIAYKYAQLADTNSNASAFKLSNSQAK 400
HPV16          1 -----MSQWIKYRCDRVDDGGDNKQIVMFLRYQG 29
ABA86972      401 IVKDCATMCRHYKRAEKKQMSMSQWIKYRCDRVDDGGDNKQIVMFLRYQG 450
HPV16          30 VEFMSFLTALKRFLQGIPKKNCILLYGAANTGKSLFGMSLMKFLQGSVIC 79
ABA86972      451 VEFMSFLTALKRFLQGIPKKNCILLYGAANTGKSLFGMSLMKFLQGSVIC 500
HPV16          80 FVNSKSHFWLQPLADAKIGMLDDATVPCWNYIDDNLRNALDGNLVSMQVK 129
ABA86972      501 FVNSKSHFWLQPLADAKIGMLDDATVPCWNYIDDNLRNALDGNLVSMQVK 550
HPV16          130 HRPLVQLKCPPLLITSNINAGTDSRWPYLHNRLVVFTFPNEFPFDENGNP 179
ABA86972      551 HRPLVQLKCPPLLITSNINAGTDSRWPYLHNRLVVFTFPNEFPFDENGNP 600
HPV16          180 VYELNDKNWKSFFSRTWSRLRL----- 201
ABA86972      601 VYELNDKNWKSFFSRTWSRLRLHEDEDKENDGDSLPTFKCVSGQNTNTL 649

```

Figure 19 The blastX program showed that recombinant E1-pMAL-c5x plasmid has highest similarity to HPV16 E1 with 100% identity.

3.5.2 Expression of recombinant E1-pMAL-c5x

Recombinant E1-pMAL plasmid was transformed into an *E. coli* BL21 (DE3) by CaCl₂ method. *E. coli* harbouring E1-pMAL-c5x plasmid were grown in LB medium containing 100 µg/ml ampicillin and E1 expression was induced by addition of 0.3 M IPTG at 37 °C. A major protein band of approximately 66 kDa appeared on 12% SDS-PAGE at highest level at 2 h post-IPTG induction (Figure 20). An estimated MW of E1-MBP fusion protein was 66 kDa. Therefore, it is likely that E1 was expressed at highest level at 2 h after IPTG induction.

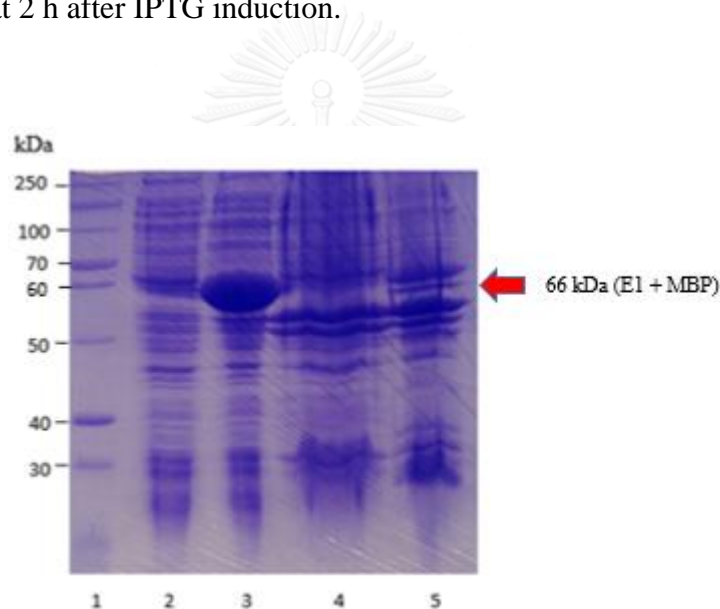


Figure 20 Expression level of recombinant HPV16 E1 protein.

Lane 1 : Unstained protein marker (Fermentas)

Lane 2 : The supernatant fraction of E1 at 0 h induction

Lane 3 : The supernatant fraction of E1 at 2 h induction

Lane 2 : The supernatant fraction of E1 at 4 h induction

Lane 3 : The supernatant fraction of E1 at 6 h induction

3.5.3 Purification of the recombinant E1-pMAL-c5x

E1-MBP fusion protein, containing his-tag at N-terminus, was purified by Ni Sepharose™ 6 Fast Flow column. Figure 21A illustrated a single protein band of 66 kDa appeared in the elution fraction. This protein was identified as E1-MBP fusion protein as it was detected by Western blot using anti-MBP antibody.

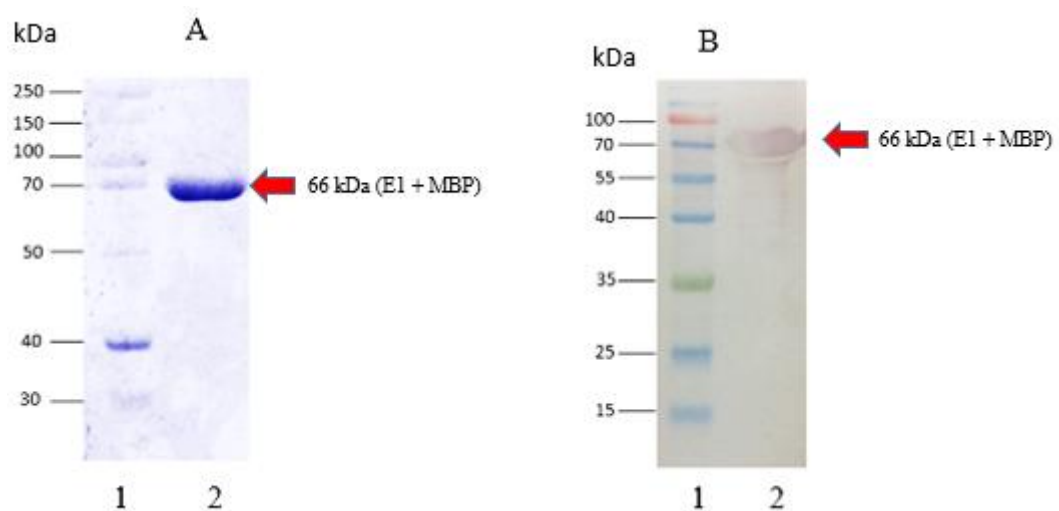


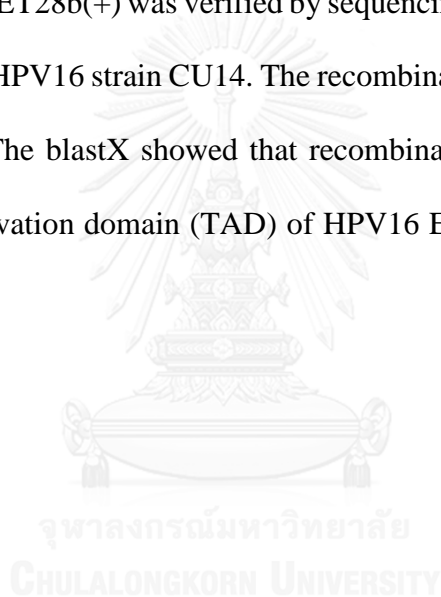
Figure 21 Purification and Western blot analysis of E1-pMAL-c5x. (A) Purification and (B) Western blot analysis of purified recombinant

- (A) Lane 1 : Unstained protein marker (Fermentas)
Lane 2 : Elution fraction of HPV16 E1 protein (500 mM imidazole)
- (B) Lane 1 : Pre-stained protein marker (Fermentas)
Lane 2 : Elution fraction of HPV16 E1 protein (500 mM imidazole)

3.6 Cloning, expression and purification of HPV16 E2

3.6.1 Construction of E2-pET28b(+)

Transactivation domain of HPV16 E2 (residues 1-201) was amplified by PCR using a viral HPV16 strain CU14 DNA as a template. PCR product was cloned into pET28b(+) vector. Recombinant E2-pET28b(+) was analyzed by *XhoI-EcoRI* digestion. Agarose gel electrophoresis revealed that E2-pET28b(+) contained an insert DNA fragment of approximately 600 bp (Figure 22). Nucleotide sequence of the inserted DNA in E2-pET28b(+) was verified by sequencing and aligned with nucleotide sequence of E2 from HPV16 strain CU14. The recombinant E2-pET28b(+) was blasted by blastX program. The blastX showed that recombinant E2-pET28b(+) has highest similarity to transactivation domain (TAD) of HPV16 E2 with 100% identity (Figure 23).



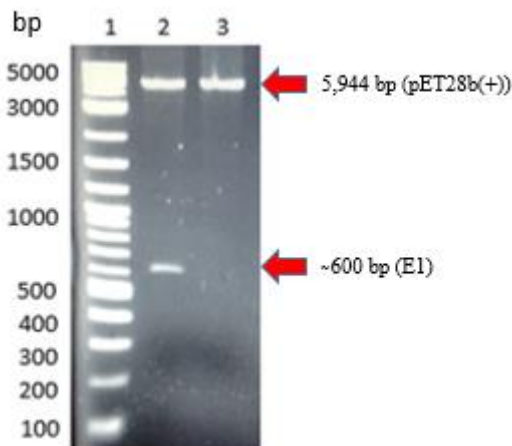
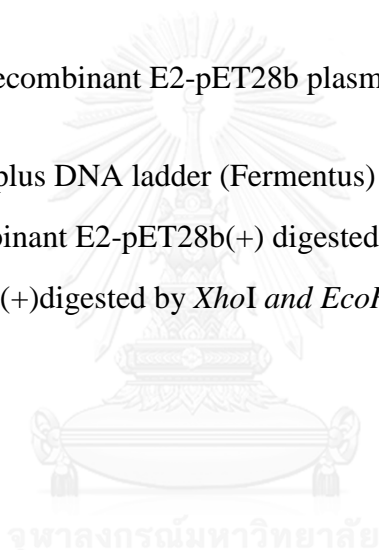


Figure 22 Analysis of recombinant E2-pET28b plasmid by *XhoI*-*EcoRI* digestion.

Lane 1 : 100 bp plus DNA ladder (Fermentus)

Lane 2 : Recombinant E2-pET28b(+) digested by *XhoI* and *EcoRI*

Lane 3 : pET28b(+) digested by *XhoI* and *EcoRI* digestion



HPV16 E2	1	METLCQRLNVCQDKILTHYENDSTNLRDHIDYWKQMRLECAIYYKAREMG	50
GenBank:AFP44250	1	METLCQRLNVCQDKILTHYENDSTNLRDHIDYWKQMRLECAIYYKAREMG	50
HPV16 E2	51	FKHINHQVVPTLAVSKNKALQAIELQLTLETIYNSQYSNEKWTLQDVSLE	100
GenBank:AFP44250	51	FKHINHQVVPTLAVSKNKALQAIELQLTLETIYNSQYSNEKWTLQDVSLE	100
HPV16 E2	101	VYLTAPTGCICKHGYTVEVQFDGDCNTMHYTNWKYIYICEETSVTVVEG	150
GenBank:AFP44250	101	VYLTAPTGCICKHGYTVEVQFDGDCNTMHYTNWKYIYICEETSVTVVEG	150
HPV16 E2	151	QVDYYGLYYVHEGIQTYFVQFKDDAEKYSKNKVWEVHAGGQVILCPTSVEF	200
GenBank:AFP44250	151	QVDYYGLYYVHEGIQTYFVQFKDDAEKYSKNKVWEVHAGGQVILCPTSVEF	200

Figure 23 The blastX program showed that recombinant E2-pET28b(+) has highest similarity to HPV16 E2 with 100% identity.

3.6.2 Expression of recombinant E2-pET28b(+)

Recombinant E2-pET28b(+) plasmid was transformed into an *E. coli* BL21 (DE3) using CaCl₂ method. Cells carrying E2-pET28b(+) plasmid was grown in LB medium containing 30 µg/ml kanamycin and E2 expression was carried out at 16 °C for 16 h. A major protein band of approximate 25 kDa was shown on 12% SDS-PAGE (Figure 24). This protein band was expected to be the E2-His tag fusion protein.

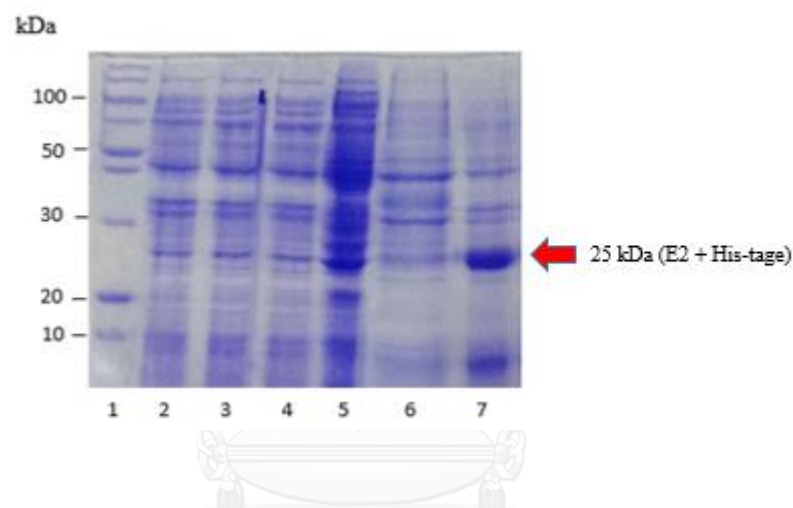


Figure 24 Expression level of recombinant HPV16 E2 protein.

Lane 1 : Unstained protein marker (Fermentus)

Lane 2 : The supernatant fraction of E2 at 0 h 37 °C induction

Lane 3 : The supernatant fraction of E2 at 2 h 37 °C induction

Lane 4 : The supernatant fraction of E2 at 4 h 37 °C induction

Lane 5 : The supernatant fraction of E2 at 6 h 37 °C induction

Lane 6 : The supernatant fraction of E2 at 0 h 16 °C induction

Lane 7 : The supernatant fraction of E2 at 16 h 16 °C induction

3.6.3 Purification of the recombinant E2/pGET28b(+)

Recombinant E2 containing 6xHis tag at the N-terminus was purified by Ni Sepharose™ 6 Fast Flow column. E2 was eluted by elution buffer containing 50 mM Tris-HCl pH 7.4, 500 mM imidazole and 300 mM NaCl. After elution step, purified E2 protein was dialyzed against 10 mM Tris-HCl, pH 7.4 and then analyzed by 12% SDS-PAGE. A major protein band presented on the gel was approximately 25 kDa. This protein band of 25 kDa was confirmed as E2 protein by Western blotting using anti-E2 antibody (Figure 25).

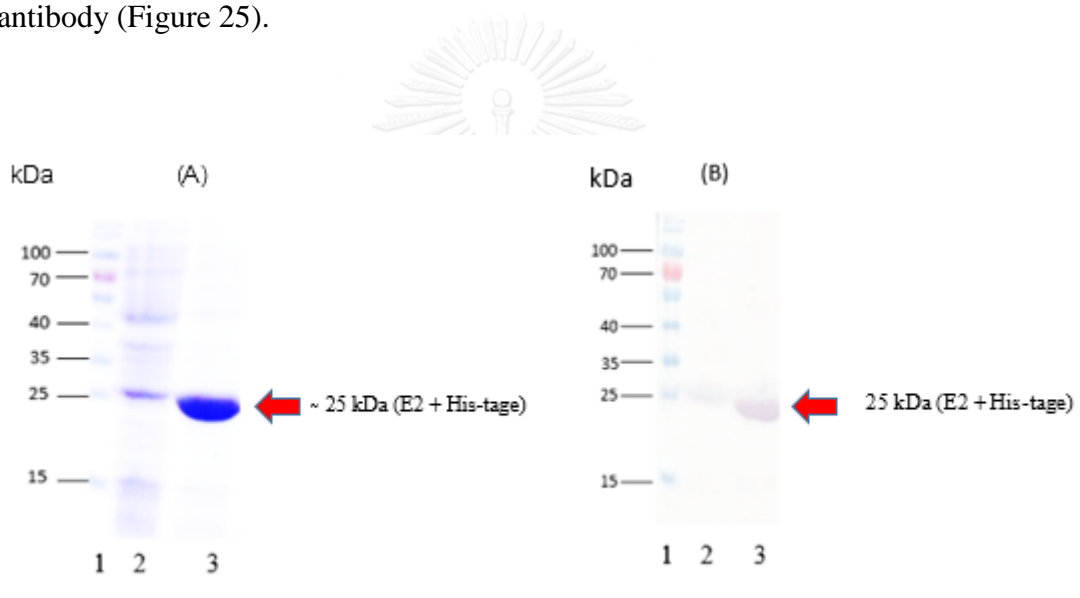


Figure 25 Purification and Western blot analysis of E2-pET28b(+). (A) Purification and (B) Western blot analysis of purified recombinant

- (A) Lane 1 : Pre-stained protein marker (Fermentas)
 Lane 2 : A flow-through protein fraction
 Lane 3 : Eluted HPV16 E2 protein
- (B) Lane 1 : Pre-stained protein marker (Fermentas)
 Lane 2 : A flow-through protein fraction
 Lane 3 : Eluted HPV16 E2 protein

3.7 Binding assays

3.7.1 Binding of HPV16 E1 and E2

Enzyme-linked immunosorbent assay (ELISA) was used to quantitatively measure of the binding of recombinant E1 and E2 protein. A microtiter plate was coated with 30 µg/ml of E2 then the excess E2 was washed out with wash buffer. The E1 was titrated with increasing concentration (0-10 µM). The data was analyzed by GraphPad Prism Version 6.0 software using nonlinearly fitting as one site – Specific binding with Hill slope model (Eq.1). Figure 26A showed that E1 bound to E2 with K_d of $8.002 \pm 0.1168 \times 10^{-6}$ M. Similar K_d of $8.880 \pm 0.1095 \times 10^{-6}$ M was determined when E1 was coated on the microtiter plate and increasing concentration of E2 was titrated to E1 (Figure 26B). This indicated that protein immobilization did not effect on protein binding. E2 was also titrated with increasing amount of MBP. However, no protein binding was observed (Figure 26C), suggesting that MBP-tag on E1-MBP fusion protein did not effect on E1-E2 binding.

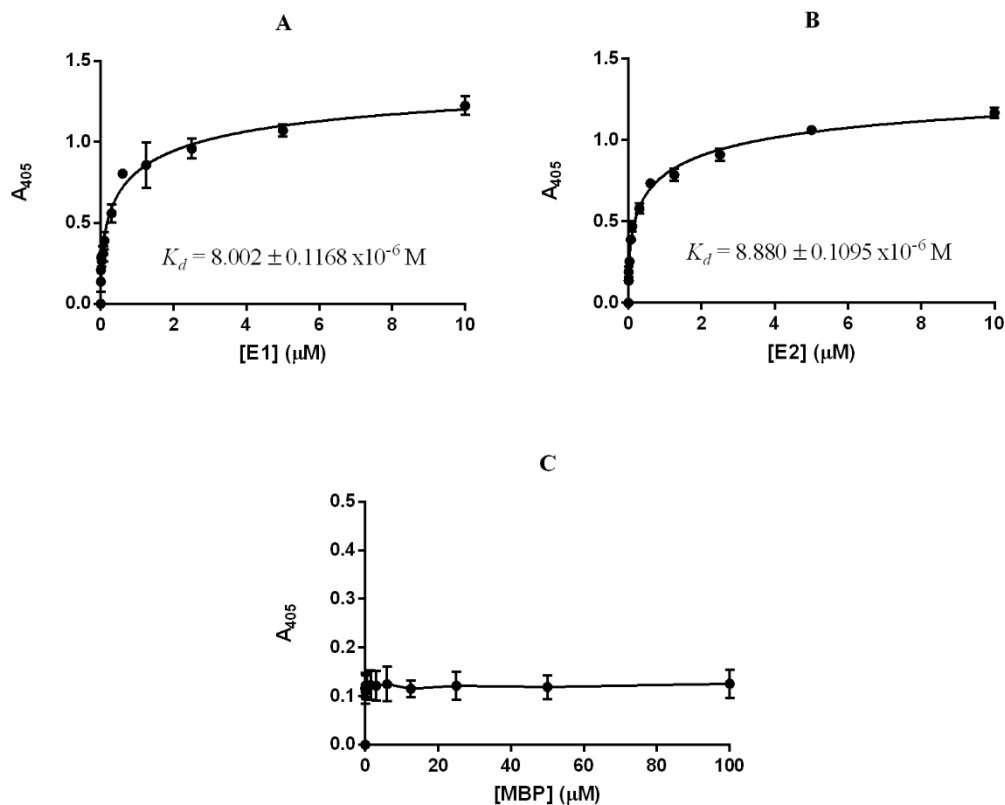


Figure 26 Quantitative binding of recombinant HPV16 E1 and E2. Recombinant HPV16 E2 was immobilized on a microplate and incubated with increasing amounts of recombinant E1 (A) or vice versa (B). The data are shown with the best fit to a nonlinearly fitting as one site – Specific binding with Hill slope. The data are given the best fit values as followed (A) $K_d = 8.002 \pm 0.1168 \times 10^{-6} \text{ M}$ and (B) $K_d = 8.880 \pm 0.1095 \times 10^{-6} \text{ M}$. (C) E2 was immobilized and titrated with increasing amounts of MBP.

3.7.2 Binding of designed peptides to HPV16 E2

ELISA used to determine binding of each designed peptide to HPV16 E2. Various concentrations of designed peptides were added to coated E2 on 96-well plate. Anti-biotin antibody was used to detect E2-peptide binding and K_d values were calculated using nonlinearly fitting as one site – Specific binding with Hill slope model (Eq.1). Figure 27 showed bindings of each designed peptides to E2. Among seven peptides, Y6R is the best E2 binder with K_d of $1.975 \pm 0.054 \mu\text{M}$, followed by W4H_Y6R and W4H with K_d of $2.842 \pm 0.073 \mu\text{M}$ and $9.457 \pm 0.138 \mu\text{M}$, respectively. Only these three peptides have lower K_d value than that of peptide4 ($12.48 \pm 0.1241 \mu\text{M}$). W4N_Y6R and W4H_Y6K have higher K_d value than that of peptide4. As shown in Figure 27, W4N_Y6R binds to E2 with K_d of $24.83 \pm 0.056 \mu\text{M}$, while W4H_Y6K binds to E2 with K_d of $21.25 \pm 0.052 \mu\text{M}$.

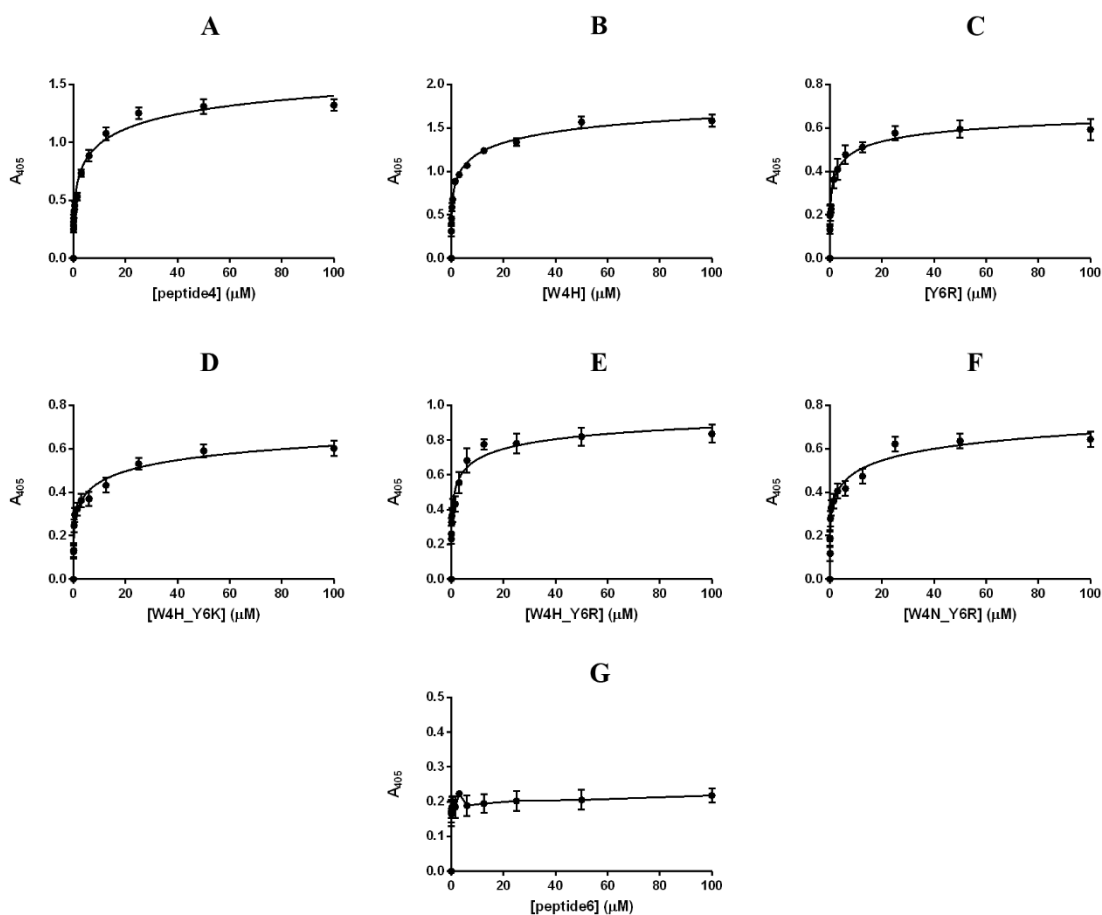


Figure 27 Quantitative binding of peptides and recombinant HPV16 E2. A constant amount of recombinant HPV16 E2 was titrated with increasing amounts of peptides: (A) peptide4 (B) W4H (C) Y6R (D) W4H_Y6K (E) W4H_Y6R (F) W4N_Y6R and (G) peptide6. The data are shown with the best fit to a nonlinearly fitting as one site – Specific binding with Hill slope. The data are given the best fit values as followed (A) peptide4, $K_d = 12.48 \pm 0.1241 \mu\text{M}$; (B) W4H, $K_d = 9.457 \pm 0.138 \mu\text{M}$; (C) Y6R, $K_d = 1.975 \pm 0.054 \mu\text{M}$; (D) W4H_Y6K, $K_d = 21.25 \pm 0.052 \mu\text{M}$; (E) W4H_Y6R, $K_d = 2.842 \pm 0.073 \mu\text{M}$; (F) W4N_Y6R, $K_d = 24.83 \pm 0.056 \mu\text{M}$; and (G) peptide6, K_d cannot be determined).

3.7.3 Determination of the inhibitory concentration 50% (IC₅₀) of designed peptides that disrupt E1-E2 binding

ELISA was used to determine inhibitory concentration 50% (IC₅₀) of designed peptides that disrupt E1-E2 binding. The recombinant E2 was fixed then titrated with various amounts of designed peptides. After washing, the excess amount of recombinant E1 was added into 96-well plate. The anti-E1 antibody was used to detect E1 and IC₅₀ values were calculated. IC₅₀ was determined by plotting the %binding of E1 against peptide concentration and fitting the data to the nonlinearly fitting as log (agonist) vs response (three parameters) (Eq.2). Figure 28 showed that Y6R, W4H and W4H_Y6R peptides had lower IC₅₀ than that of peptide4, indicating that Y6R, W4H and W4H_Y6R peptides have greater potential to inhibit E1-E2 complex formation than peptide4 (Table 11).

Table 11 summarized the properties of peptides inhibitors. Among seven peptides, Y6R peptide is the best E2 binder with K_d of $1.975 \pm 0.054 \mu\text{M}$ and gave the lowest binding energy to E2 (-830.8 kcal/mol), followed by W4H_Y6R and W4H with K_d of $2.842 \pm 0.073 \mu\text{M}$ and the lowest binding energy to E2 of -791.1 kcal/mol and K_d of $9.457 \pm 0.138 \mu\text{M}$ and the lowest binding energy to E2 of -777 kcal/mol , respectively. These three peptides showed a higher affinity interaction to E2 than peptide4 (K_d of peptide4, $12.48 \pm 0.1241 \mu\text{M}$). This corresponds to the fact that W4H, Y6R and W4H_Y6R have lower IC₅₀ value than that of peptide4. In contrast, W4N_Y6R and W4H_Y6K have higher K_d than that of that peptide4. W4N_Y6R is the worst E2 binder among newly designed peptides with K_d of $24.83 \pm 0.056 \mu\text{M}$, followed by W4H_Y6K with K_d of $21.25 \pm 0.052 \mu\text{M}$. These two peptides inhibited E1 and E2 with higher IC₅₀

value. W4H_Y6K and W4N_Y6R inhibited E1 and E2 with IC_{50} of $0.4418 \pm 0.147 \mu\text{M}$ and $0.7805 \pm 0.114 \mu\text{M}$, respectively.

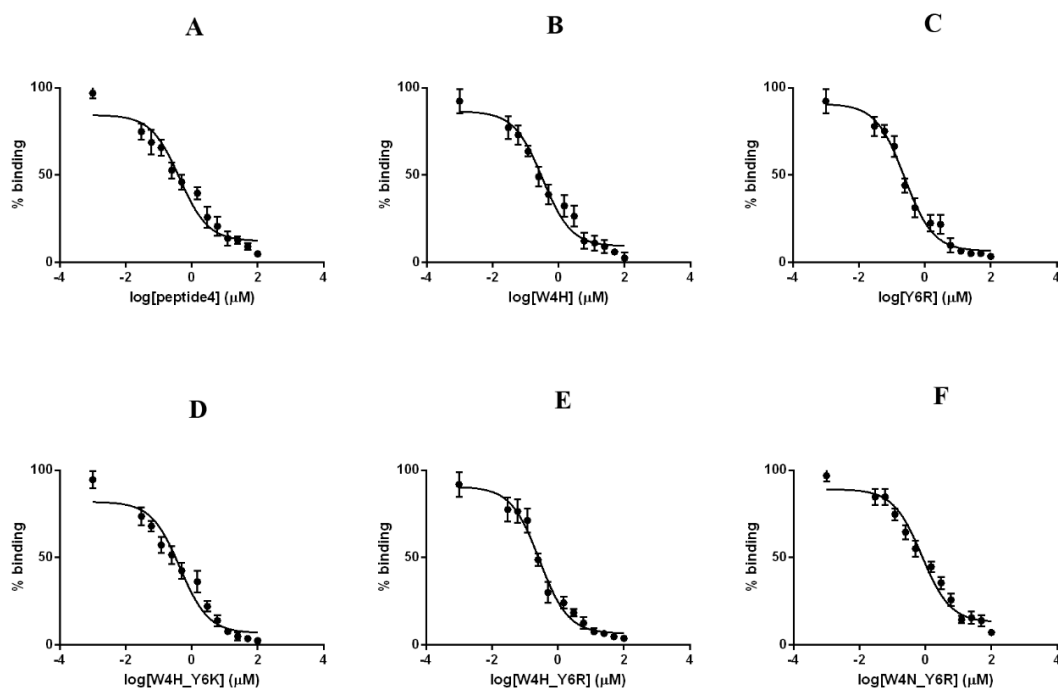


Figure 28 Concentration-response curves of peptides that inhibit E1-E2 binding. Inhibitory activity of peptide4 (A), W4H (B), Y6R (C), W4H_Y6K (D), W4H_Y6R (E) and W4N_Y6R (F) was determined by a nonlinearly fitting as log(agonist) vs response (three parameters). IC_{50} , a designed peptide concentration (μM) that inhibits 50% of E1 and E2 binding.

Table 11 Properties of peptide inhibitors.

Peptide	Binding energy ^[a] (kcal/mol)	Dissociation constant ^[b] (μ M)	IC ₅₀ ^[c] (μ M)
Peptide-4	-713.6	12.48 \pm 0.1241	0.4293 \pm 0.154
W4H	-777.0	9.457 \pm 0.138	0.3292 \pm 0.129
Y6R	-830.8	1.975 \pm 0.054	0.2443 \pm 0.093
W4H_Y6K	-739.1	21.25 \pm 0.052	0.4418 \pm 0.147
W4H_Y6R	-791.1	2.842 \pm 0.073	0.2781 \pm 0.095
W4N_Y6R	-744.5	24.83 \pm 0.056	0.7805 \pm 0.114
Peptide-6	-519.4	-	-

^[a] Binding energy (kcal/mol) of peptide to HPV16 E2

^[b] Dissociation constant, K_d , of peptide and HPV16 E2 binding

^[c] IC₅₀, a concentration (μ M) of peptide that inhibits 50% of E1 and E2 complex.

CHAPTER IV

DISCUSSION

Cancer is the most leading cause of death worldwide. It was expected that the number of deaths from cancer will continue growing. Cancers have many characteristics such as uncontrolled growth, spread of cells death, escaping the host immune system, and others. There are several cancer treatment methods such as chemotherapy, radiotherapy and surgical treatment. These treatment methods mainly focus on mass cell killing without high specificity and have many side effects. Peptide therapy has many advantages, including specific to target cancer cell, rapid clearance from the blood and low toxicity. Identification and development of anti-cancer peptides provide good opportunities for prevention and treatment.

The main cause of cervical cancer, the second leading cause of death in women worldwide, is HPV infection. HPV16 E2 plays an important role in viral gene regulation. Previously, Fujii et al., 2003 reported that small peptide inhibitor screened by phage display library could bind to HPV16 E2 and inhibited the transcriptional regulatory function of E2 in a tested cell line. This research aims to design novel peptides with improved properties to binding to HPV16 E2 and disrupt the E1-E2 complex formation.

Structure of HPV16 E2 (residue 1-201) was built and minimized. Figure 11A shown the superimposition of the structures HPV16 E2 and HPV18 E2 with high structural similarity, RMSD = 1.31 Å. Since the crystal structure of HPV16 E1-E2

complex was not available, the models of HPV16 E1 (residues 421-622) were created by I-TASSER server. The model with the best C-score was selected for docking onto the structure of HPV16 E2 using ClusPro. Superimposition of the predicted structure of HPV16 E1 and the crystal structure of HPV18 E1 gave low RMSD value (1.39 Å), indicating their structural similarity. The structure of the predicted HPV16 E1-E2 complex was also similar to the crystal structure of HPV18 E1-E2 complex, with RMSD = 1.11 Å.

The docked HPV16 E1-E2 complex revealed that there are three interacting sites for HPV16 E1 and E2 complex (β -strand structural domain of HPV16 E2, N-terminal helical domain of HPV16 E2 and helical linker segment between the N-terminal and C-terminal domains of HPV16 E2, Figure 12A). Figure 12B shown hydrogen bonds on β -strand domain of HPV16 E2 residues Glu118, Asn127, Met129, Tyr178 with Tyr578, Arg575, Ser574, Asp573 of HPV16 E1, respectively. Major contact site of E1 and E2, where Asp13, Thr17, Tyr19, Asp22, Tyr32, Glu39, Val58 of HPV16 E2 form hydrogen bonds with Arg615 (to Asp13 and Thr17 of E2), Arg447, Arg619, Glu452, Arg447, Tyr602 of HPV16 E1, respectively (Figure 12C and D). Gln95 and Glu100, on the helical linker segment of HPV16 E2, form hydrogen bond with Arg462 and Ser455 of HPV16 E1.

The structures of nine peptides reported in Fujii et al, 2003 were constructed by I-TASSER server. All of these peptides had C-scores better than -1.5, indicating that all models have correct topologies. ClusPro was used to dock these peptides to HPV16 E2 than predict binding interactions. Peptide4 was calculated as lowest binding energy

correlated with highest A value in previous experimental, indicating that it was the best E2 binder. The trend the binding energy of each nine peptides were also reasonably correlated with the trend of the previous experimental A values (Table 9).

Peptide4 was predicted binding conformation and interactions within the E1-E2 interface. Residues of peptide4, TYR6 was predicted to form a hydrogen bond with M36 of E2 and TYR8 was predicted to form hydrogen bonds with Q12 and E39 of E2 (Figure 14). Abbate et al, 2004 reported that E39 of HPV18 E2 is the key residue for the interaction with helicase domain of E1. The interaction between TYR8 of peptide4 with E39 of HPV16 may be one of the most important factors that contribute to peptide4 have high efficiency to bind to E2 and disrupt E1-E2 complex formation.

Peptide inhibitor that could form hydrogen bonds to E2 and also disrupt interactions between E1 and E2 complex formation was designed base on peptide4. TRP4 and TYR6 of peptide4 were predicted to have potentially obstruct the binding interactions between HPV16 E1 and E2. TRP4 was mutated to His, Asn, Ser (Figure 15) and TYR6 was mutated to Lys, Asn, Arg (Figure 16). All possible mutated peptides were constructed by I-TASSER server and docked onto HPV16 E2. Only five peptides (W4H, W4H_Y6K, W4H_Y6R, W4N_Y6R and Y6R) gave the binding energy lower than that of peptide4 and located within E1-E2 interface. W4H_Y6K, W4N_Y6R and Y6R were predicted to form four hydrogen bonds with E2 protein, while W4H and W4H_Y6R were predicted to form five hydrogen bonds. Presumably, these five peptides could potentially bind to HPV16 E2 better than peptide4 did (peptide4 was predicted to bind to E2 with three hydrogen bonds).

Recombinant HPV16 E1 and E2 proteins were expressed. HPV16 E1 has MBP-tag at the N-terminus, in order to enhance the solubility of E1; and it also contains C-terminal his-tag to ease purification. Meanwhile, HPV16 E2 was expressed as N-terminal his-tag fusion protein. Recombinant HPV16 E1 and E2 proteins were purified by a Ni-NTA column and eluted with a solution containing 500 mM imidazole. Recombinant HPV16 E1 and E2 were eluted as major protein band of approximately 66 kDa and 25 kDa (Figure 21A and 21A, respectively). Both recombinant proteins were confirmed by Western immunoblotting using rabbit anti-His antibody and mouse anti-E2 antibody as primary antibody, respectively (Figure 21B and 25B). Recombinant HPV16 E1 and E2 were then used in binding experiments.

ELISA was used to determine binding of recombinant HPV16 E2 and E1. Figure 26 showed binding similarity of E1 to E2 and E2 to E1 with apparent K_d of $(8.002 \pm 0.1168) \times 10^{-6}$ M and K_d of $(8.880 \pm 0.1095) \times 10^{-6}$ M, respectively (Figure 26A and B). This result indicated that immobilizing either E1 or E2 on a microplate did not affect E1-E2 binding. Figure 26C showed no binding of MBP and E2, indicating that MBP tag did not affect E2 binding.

The K_d and IC_{50} values were determined by ELISA. In Figure 27 and 28, peptide4 bound to recombinant E2 with a K_d of 12.48 ± 0.1241 μ M while peptide6 (negative control) showed no binding to E2 protein. In addition, three designed peptides Y6R, W4H_Y6R and W4H showed higher binding affinities to E2 protein than peptide4 (Y6R, $K_d = 1.975 \pm 0.054$ μ M; W4H_Y6R, $K_d = 2.842 \pm 0.073$ μ M; and W4H, $K_d = 9.457 \pm 0.138$ μ M). Figure 28 showed Y6R, W4H_Y6R and W4H peptides had

lower IC_{50} than that of peptide4, indicating that Y6R, W4H_Y6R and W4H peptides possess higher efficiency to inhibit E1-E2 complex formation than peptide4.

Table 11 summarizes properties of peptides used in this study. Y6R peptide gave the lowest binding energy to E2 (-830.8 kcal/mol), followed by W4H_Y6R (-791.1 kcal/mol) and W4H (-777 kcal/mol). These three peptides also showed a high-affinity interaction to E2, Y6R have higher binding affinities to E2 with lowest K_d value, followed by W4H_Y6R and W4H, respectively. In addition; Y6R, W4H_Y6R and W4H peptides possess lower IC_{50} than peptide4, suggesting that these three peptides are stronger inhibitors than peptide4. This may be due to the fact that Y6R, W4H_Y6R and W4H peptides form many hydrogen bonds to E2 protein.

Wang et al., 2004 reported that Glu100, Tyr19, His32 and Lue94 of HPV11 E2, form a deep hydrophobic pocket for indandione inhibitor. Figure 17 showed binding conformation and interaction of designed peptides within E1 and E2. All of designed were predicted to contact with E1 protein in this area. For this reason, all of peptides have effective for inhibition of E1-E2.

In previous study, Glu43 of HPV18 E2 was key residue for replication of E2 (Ferguson and Botchan, 1996, Harris and Botchan, 1999). E43 of HPV18 E2 is in favourable ionic interaction with R454. Mutation of E43 of E2 or R454 of E1 had result in reduction of E1-E2 complex formation of HPV18. E43 of HPV18 E2 is corresponding to E39 in HPV16. HIS10 of W4H and ARG6 of W4H_Y6R peptides were also predicted to form hydrogen bonds with E39 of HPV16 E2 (Figure 17A and

C, respectively). These results emphasized the importance of ARG6 and HIS10 residues in these peptides inhibitors.

Fujii et al, 2003 demonstrated that the tryptophan-rich sequence in peptide4 was important for E2 protein binding. However, this results showed that W4H peptide (TWFHPYPYPHLP) exhibited higher affinity for E2 protein than peptide4 (TWFWPYPYPHLP). W4H peptide was predicted to potentially form five hydrogen bonds to E2 protein (Figure 17A) while peptide4 was predicted to interact with E2 with three hydrogen bonds (Figure 14). In addition, Y6R peptide (best peptide inhibitor in this study) was predicted to form only four hydrogen bonds with E2 protein (Figure 17E). Presumably, Y6R may have favorable van der Waals interactions with nearby residues of E2. This result suggested that various interactions were involved in the binding between the peptides and E2. Therefore, all possible interactions should be considered for designing effective peptide inhibitors.

Several antiviral have been evaluated as treatment for HPV-associated cervical lesions. Cidofovir is an acyclic nucleoside phosphonate derivative, which has broad-spectrum activity against DNA viruses (Snoeck et al., 2000). Podophyllin is cytotoxic agent, which arrests mitosis in metaphase. This agent suppressed HPV gene expression and cell growth in cervical cancer cell lines (Okamoto et al., 1999). IFN- α is approved for treatment of genital warts (Cirelli and Tyring, 1994), which produced by leukocytes. They are mainly involved in innate immune response against viral infection. However, these anti-HPV drugs are easily lead to liver and kidney damage, and produce drug resistance after prolonged treatment (Wang et al., 2014). Therefore, the development

of novel peptide therapeutics with high specificity, high affinity, low toxicity, is very importance.



CHAPTER V

CONCLUSIONS

In this study, the binding conformations and interactions between the small peptides and HPV16 E2 were predicted and analyzed. The ranking of the predicted binding affinities is reasonably in agreement with previous experimental results (Fujii et al., 2003).

HPV16 E1 and E2 gene were successfully cloned and recombinant proteins were expressed and purified. HPV16 E1 and E2 were eluted as major protein band of approximately 66 kDa and 25 kDa, respectively. Both recombinant proteins were confirmed as recombinant E1 and E2 by Western immunoblotting using anti-His antibody and anti-E2 antibody, respectively.

Based on Fuji et al., 2003 , peptide4 was the best E2 binder. Therefore, peptide inhibitor was designed based on peptide4. TRP4 and TYR6 of peptide4 were mutated into all possible 20 amino acids. Only newly designed five peptides (W4H, W4H_Y6K, W4H_Y6R, W4N_Y6R and Y6R) showed the lowest binding energies of the largest clusters lower than peptide4.

In binding experiments, Y6R, W4H_Y6R and W4H showed higher binding affinities to E2 protein than that of peptide4 (Peptide 4, $K_d =$; Y6R, $K_d = 1.975 \pm 0.054 \mu\text{M}$; W4H_Y6R, $K_d = 2.842 \pm 0.073 \mu\text{M}$; and W4H, $K_d = 9.457 \pm 0.138 \mu\text{M}$). In addition, Y6R, W4H_Y6R and W4H showed higher efficiency to inhibit E1-E2 complex

formation than peptide4 (Peptide4, $IC_{50} = 0.4293 \pm 0.154 \mu\text{M}$; Y6R, $IC_{50} = 0.2443 \pm 0.093 \mu\text{M}$, W4H_Y6R, $IC_{50} = 0.2781 \pm 0.095 \mu\text{M}$ and W4H, $IC_{50} = 0.3292 \pm 0.129 \mu\text{M}$).



REFERENCES

- ABBATE, E. A., BERGER, J. M. & BOTCHAN, M. R. 2004. The X-ray structure of the papillomavirus helicase in complex with its molecular matchmaker E2. *Genes Dev*, 18, 1981-96.
- ALONSO, A. & REED, J. 2002. Modelling of the human papillomavirus type 16 E5 protein. *Biochim Biophys Acta*, 1601, 9-18.
- AMIN, A. A., TITOLO, S., PELLETIER, A., FINK, D., CORDINGLEY, M. G. & ARCHAMBAULT, J. 2000. Identification of domains of the HPV11 E1 protein required for DNA replication in vitro. *Virology*, 272, 137-50.
- ANTSON, A. A., BURNS, J. E., MOROZ, O. V., SCOTT, D. J., SANDERS, C. M., BRONSTEIN, I. B., DODSON, G. G., WILSON, K. S. & MAITLAND, N. J. 2000. Structure of the intact transactivation domain of the human papillomavirus E2 protein. *Nature*, 403, 805-9.
- ARBYN, M., DE SANJOSE, S., SARAIYA, M., SIDERI, M., PALEFSKY, J., LACEY, C., GILLISON, M., BRUNI, L., RONCO, G., WENTZENSEN, N., BROTHERTON, J., QIAO, Y. L., DENNY, L., BORNSTEIN, J., ABRAMOWITZ, L., GIULIANO, A., TOMMASINO, M. & MONSONEGO, J. 2012. EUROGIN 2011 roadmap on prevention and treatment of HPV-related disease. *Int J Cancer*, 131, 1969-82.
- AUSTER, A. S. & JOSHUA-TOR, L. 2004. The DNA-binding domain of human papillomavirus type 18 E1. Crystal structure, dimerization, and DNA binding. *J Biol Chem*, 279, 3733-42.
- BERGVALL, M., MELENDY, T. & ARCHAMBAULT, J. 2013. The E1 proteins. *Virology*, 445, 35-56.
- BERNARD, H. U. 2013. Regulatory elements in the viral genome. *Virology*, 445, 197-204.
- BERNARD, H. U., BURK, R. D., CHEN, Z., VAN DOORSLAER, K., ZUR HAUSEN, H. & DE VILLIERS, E. M. 2010. Classification of papillomaviruses (PVs) based on 189 PV types and proposal of taxonomic amendments. *Virology*, 401, 70-9.
- BOSCH, F. X., BURCHELL, A. N., SCHIFFMAN, M., GIULIANO, A. R., DE SANJOSE, S., BRUNI, L., TORTOLERO-LUNA, G., KJAER, S. K. & MUNOZ, N. 2008. Epidemiology and natural history of human papillomavirus infections and type-specific implications in cervical neoplasia. *Vaccine*, 26 Suppl 10, K1-16.
- BRENTJENS, M. H., YEUNG-YUE, K. A., LEE, P. C. & TYRING, S. K. 2002. Human papillomavirus: a review. *Dermatol Clin*, 20, 315-31.
- BURD, E. M. 2003. Human Papillomavirus and Cervical Cancer. *Clin Microbiol Rev*, 16, 1-17.
- CHAN, P. K., CHANG, A. R., YU, M. Y., LI, W. H., CHAN, M. Y., YEUNG, A. C., CHEUNG, T. H., YAU, T. N., WONG, S. M., YAU, C. W. & NG, H. K. 2010. Age distribution of human papillomavirus infection and cervical neoplasia reflects caveats of cervical screening policies. *Int J Cancer*, 126, 297-301.
- CHEN, G. & STENLUND, A. 1998. Characterization of the DNA-binding domain of the bovine papillomavirus replication initiator E1. *J Virol*, 72, 2567-76.

- CIRELLI, R. & TYRING, S. K. 1994. Interferons in human papillomavirus infections. *Antiviral Res*, 24, 191-204.
- CLIFFORD, G. M., RANA, R. K., FRANCESCHI, S., SMITH, J. S., GOUGH, G. & PIMENTA, J. M. 2005. Human papillomavirus genotype distribution in low-grade cervical lesions: comparison by geographic region and with cervical cancer. *Cancer Epidemiol Biomarkers Prev*, 14, 1157-64.
- COMEAU, S. R., GATCHELL, D. W., VAJDA, S. & CAMACHO, C. J. 2004. ClusPro: a fully automated algorithm for protein-protein docking. *Nucleic Acids Res*, 32, W96-9.
- CRAIK, D. J., FAIRLIE, D. P., LIRAS, S. & PRICE, D. 2013. The future of peptide-based drugs. *Chem Biol Drug Des*, 81, 136-47.
- CUBIE, H. A. 2013. Diseases associated with human papillomavirus infection. *Virology*, 445, 21-34.
- D'ABRAMO, C. & ARCHAMBAULT, J. 2011. Small Molecule Inhibitors of Human Papillomavirus Protein - Protein Interactions. *Open Virol J*, 5, 80-95.
- DE SANJOSE, S., DIAZ, M., CASTELLSAGUE, X., CLIFFORD, G., BRUNI, L., MUNOZ, N. & BOSCH, F. X. 2007. Worldwide prevalence and genotype distribution of cervical human papillomavirus DNA in women with normal cytology: a meta-analysis. *Lancet Infect Dis*, 7, 453-9.
- DE VILLIERS, E. M. 2013. Cross-roads in the classification of papillomaviruses. *Virology*, 445, 2-10.
- DE VILLIERS, E. M., FAUQUET, C., BROKER, T. R., BERNARD, H. U. & ZUR HAUSEN, H. 2004. Classification of papillomaviruses. *Virology*, 324, 17-27.
- DIAZ, M. L. 2008. Human papilloma virus: prevention and treatment. *Obstet Gynecol Clin North Am*, 35, 199-217, vii-viii.
- DIXON, E. P., PAHEL, G. L., ROCQUE, W. J., BARNES, J. A., LOBE, D. C., HANLON, M. H., ALEXANDER, K. A., CHAO, S. F., LINDLEY, K. & PHELPS, W. C. 2000. The E1 helicase of human papillomavirus type 11 binds to the origin of replication with low sequence specificity. *Virology*, 270, 345-57.
- DOLINSKY, T. J., NIELSEN, J. E., MCCAMMON, J. A. & BAKER, N. A. 2004. PDB2PQR: an automated pipeline for the setup of Poisson-Boltzmann electrostatics calculations. *Nucleic Acids Res*, 32, W665-7.
- EDWARDS, C. M., COHEN, M. A. & BLOOM, S. R. 1999. Peptides as drugs. *Qjm*, 92, 1-4.
- FERGUSON, M. K. & BOTCHAN, M. R. 1996. Genetic analysis of the activation domain of bovine papillomavirus protein E2: its role in transcription and replication. *J Virol*, 70, 4193-9.
- FERLAY, J., SHIN, H. R., BRAY, F., FORMAN, D., MATHERS, C. & PARKIN, D. M. 2010. Estimates of worldwide burden of cancer in 2008: GLOBOCAN 2008. *Int J Cancer*, 127, 2893-917.
- FRAZER, I. H., LEGGATT, G. R. & MATTAROLLO, S. R. 2011. Prevention and treatment of papillomavirus-related cancers through immunization. *Annu Rev Immunol*, 29, 111-38.
- FUJII, T., AUSTIN, D., GUO, D., SRIMATKANDADA, S., WANG, T., KUBUSHIRO, K., MASUMOTO, N., TSUKAZAKI, K., NOZAWA, S. &

- DEISSEROTH, A. B. 2003. Peptides inhibitory for the transcriptional regulatory function of human papillomavirus E2. *Clin Cancer Res*, 9, 5423-8.
- GNANAMONY, M., PEEDICAYIL, A. & ABRAHAM, P. 2007. An overview of human papillomaviruses and current vaccine strategies. *Indian J Med Microbiol*, 25, 10-7.
- GUEX, N. & PEITSCH, M. C. 1997. SWISS-MODEL and the Swiss-PdbViewer: an environment for comparative protein modeling. *Electrophoresis*, 18, 2714-23.
- HARRIS, S. F. & BOTCHAN, M. R. 1999. Crystal structure of the human papillomavirus type 18 E2 activation domain. *Science*, 284, 1673-7.
- HILDESHEIM, A., HERRERO, R., WACHOLDER, S., RODRIGUEZ, A. C., SOLOMON, D., BRATTI, M. C., SCHILLER, J. T., GONZALEZ, P., DUBIN, G., PORRAS, C., JIMENEZ, S. E. & LOWY, D. R. 2007. Effect of human papillomavirus 16/18 L1 viruslike particle vaccine among young women with preexisting infection: a randomized trial. *Jama*, 298, 743-53.
- HORVATH, C. A., BOULET, G. A., RENOUX, V. M., DELVENNE, P. O. & BOGERS, J. P. 2010. Mechanisms of cell entry by human papillomaviruses: an overview. *Viol J*, 7, 11.
- JONES, H. W., 3RD 2000. Clinical treatment of women with atypical squamous cells of undetermined significance or atypical glandular cells of undetermined significance cervical cytology. *Clin Obstet Gynecol*, 43, 381-93.
- KAJITANI, N., SATSUKA, A., KAWATE, A. & SAKAI, H. 2012. Productive Lifecycle of Human Papillomaviruses that Depends Upon Squamous Epithelial Differentiation. *Front Microbiol*, 3, 152.
- KIM, S. S., TAM, J. K., WANG, A. F. & HEGDE, R. S. 2000. The structural basis of DNA target discrimination by papillomavirus E2 proteins. *J Biol Chem*, 275, 31245-54.
- LIU, Y., YOU, H., CHIRIVA-INTERNATI, M., KOROURIAN, S., LOWERY, C. L., CAREY, M. J., SMITH, C. V. & HERMONAT, P. L. 2001. Display of complete life cycle of human papillomavirus type 16 in cultured placental trophoblasts. *Virology*, 290, 99-105.
- LONGWORTH, M. S. & LAIMINS, L. A. 2004. Pathogenesis of Human Papillomaviruses in Differentiating Epithelia. *Microbiol Mol Biol Rev*, 68, 362-72.
- MCBRIDE, A. A. 2013. The Papillomavirus E2 proteins. *Virology*, 445, 57-79.
- MCKINNEY, C. C., HUSSMANN, K. L. & MCBRIDE, A. A. 2015. The Role of the DNA Damage Response throughout the Papillomavirus Life Cycle. *Viruses*, 7, 2450-69.
- MEYERS, C., BROMBERG-WHITE, J. L., ZHANG, J., KAUPAS, M. E., BRYAN, J. T., LOWE, R. S. & JANSEN, K. U. 2002. Infectious Virions Produced from a Human Papillomavirus Type 18/16 Genomic DNA Chimera. *J Virol*, 76, 4723-33.
- MONTZ, F. J. 2000. Management of high-grade cervical intraepithelial neoplasia and low-grade squamous intraepithelial lesion and potential complications. *Clin Obstet Gynecol*, 43, 394-409.
- MORIN, G., FRADET-TURCOTTE, A., DILELLO, P., BERGERON-LABRECQUE, F., OMICHINSKI, J. G. & ARCHAMBAULT, J. 2011. A conserved

- amphipathic helix in the N-terminal regulatory region of the papillomavirus E1 helicase is required for efficient viral DNA replication. *J Virol*, 85, 5287-300.
- MUNGER, K., SCHEFFNER, M., HUIBREGTSE, J. M. & HOWLEY, P. M. 1992. Interactions of HPV E6 and E7 oncoproteins with tumour suppressor gene products. *Cancer Surv*, 12, 197-217.
- MUNOZ, N., BOSCH, F. X., DE SANJOSE, S., HERRERO, R., CASTELLSAGUE, X., SHAH, K. V., SNIJDERS, P. J. & MEIJER, C. J. 2003. Epidemiologic classification of human papillomavirus types associated with cervical cancer. *N Engl J Med*, 348, 518-27.
- MUNOZ, N., CASTELLSAGUE, X., DE GONZALEZ, A. B. & GISSMANN, L. 2006. Chapter 1: HPV in the etiology of human cancer. *Vaccine*, 24 Suppl 3, S3/1-10.
- NARECHANIA, A., TERAJ, M. & BURK, R. D. 2005. Overlapping reading frames in closely related human papillomaviruses result in modular rates of selection within E2. *J Gen Virol*, 86, 1307-13.
- OKAMOTO, A., WOODWORTH, C. D., YEN, K., CHUNG, J., ISONISHI, S., NIKAIDO, T., KIYOKAWA, T., SEO, H., KITAHARA, Y., OCHIAI, K. & TANAKA, T. 1999. Combination therapy with podophyllin and vidarabine for human papillomavirus positive cervical intraepithelial neoplasia. *Oncol Rep*, 6, 269-76.
- PINTO, A. P. & CRUM, C. P. 2000. Natural history of cervical neoplasia: defining progression and its consequence. *Clin Obstet Gynecol*, 43, 352-62.
- RAJ, K., BERGUERAND, S., SOUTHERN, S., DOORBAR, J. & BEARD, P. 2004. E1(Δ)E4 Protein of Human Papillomavirus Type 16 Associates with Mitochondria. *J Virol*, 78, 7199-207.
- RANK, N. M. & LAMBERT, P. F. 1995. Bovine papillomavirus type 1 E2 transcriptional regulators directly bind two cellular transcription factors, TFIID and TFIIB. *J Virol*, 69, 6323-34.
- ROSENBLATT, C., LUCON, A. M., PEREYRA, E. A., PINOTTI, J. A., ARAP, S. & RUIZ, C. A. 2004. HPV prevalence among partners of women with cervical intraepithelial neoplasia. *Int J Gynaecol Obstet*, 84, 156-61.
- ROY, A., KUCUKURAL, A. & ZHANG, Y. 2010. I-TASSER: a unified platform for automated protein structure and function prediction. *Nat Protoc*, 5, 725-38.
- SANCLEMENTE, G. & GILL, D. K. 2002. Human papillomavirus molecular biology and pathogenesis. *J Eur Acad Dermatol Venereol*, 16, 231-40.
- SANDERS, C. M., KOVALEVSKIY, O. V., SIZOV, D., LEBEDEV, A. A., ISUPOV, M. N. & ANTSON, A. A. 2007. Papillomavirus E1 helicase assembly maintains an asymmetric state in the absence of DNA and nucleotide cofactors. *Nucleic Acids Res*, 35, 6451-7.
- SAPP, M. & BIENKOWSKA-HABA, M. 2009. Viral entry mechanisms: human papillomavirus and a long journey from extracellular matrix to the nucleus. *Febs j*, 276, 7206-16.
- SCHLEGEL, R., PHELPS, W. C., ZHANG, Y. L. & BARBOSA, M. 1988. Quantitative keratinocyte assay detects two biological activities of human papillomavirus DNA and identifies viral types associated with cervical carcinoma. *Embo j*, 7, 3181-7.

- SEKHAR, V., REED, S. C. & MCBRIDE, A. A. 2010. Interaction of the betapapillomavirus E2 tethering protein with mitotic chromosomes. *J Virol*, 84, 543-57.
- SHAH, K. V. & BUSCEMA, J. 1988. Genital warts, papillomaviruses, and genital malignancies. *Annu Rev Med*, 39, 371-9.
- SIRITANTIKORN, S., LAIWEJPITHAYA, S., SIRIPANYAPHINYO, U., AUEWARAKUL, P., YENCHITSOMANUS, P., THAKERNPOL, K. & WASI, C. 1997. Detection and typing of human papilloma virus DNAs in normal cervix, intraepithelial neoplasia and cervical cancer in Bangkok. *Southeast Asian J Trop Med Public Health*, 28, 707-10.
- SNOECK, R., NOEL, J. C., MULLER, C., DE CLERCQ, E. & BOSSENS, M. 2000. Cidofovir, a new approach for the treatment of cervix intraepithelial neoplasia grade III (CIN III). *J Med Virol*, 60, 205-9.
- STUBENRAUCH, F. & LAIMINS, L. A. 1999. Human papillomavirus life cycle: active and latent phases. *Semin Cancer Biol*, 9, 379-86.
- STUNKEL, W. & BERNARD, H. U. 1999. The chromatin structure of the long control region of human papillomavirus type 16 represses viral oncoprotein expression. *J Virol*, 73, 1918-30.
- TAN, S. H., LEONG, L. E., WALKER, P. A. & BERNARD, H. U. 1994. The human papillomavirus type 16 E2 transcription factor binds with low cooperativity to two flanking sites and represses the E6 promoter through displacement of Sp1 and TFIID. *J Virol*, 68, 6411-20.
- THIERRY, F. 2009. Transcriptional regulation of the papillomavirus oncogenes by cellular and viral transcription factors in cervical carcinoma. *Virology*, 384, 375-379.
- TITOLO, S., BRAULT, K., MAJEWSKI, J., WHITE, P. W. & ARCHAMBAULT, J. 2003. Characterization of the minimal DNA binding domain of the human papillomavirus e1 helicase: fluorescence anisotropy studies and characterization of a dimerization-defective mutant protein. *J Virol*, 77, 5178-91.
- TUREK, L. P. 1994. The Structure, Function, and Regulation of Papillomaviral Genes in Infection and Cervical Cancer. In: KARL MARAMOROSCH, F. A. M. & AARON, J. S. (eds.) *Advances in Virus Research*. Academic Press.
- VAN KRIEKINGE, G., CASTELLSAGUE, X., CIBULA, D. & DEMARTEAU, N. 2014. Estimation of the potential overall impact of human papillomavirus vaccination on cervical cancer cases and deaths. *Vaccine*, 32, 733-9.
- WALBOOMERS, J. M., JACOBS, M. V., MANOS, M. M., BOSCH, F. X., KUMMER, J. A., SHAH, K. V., SNIJDERS, P. J., PETO, J., MEIJER, C. J. & MUNOZ, N. 1999. Human papillomavirus is a necessary cause of invasive cervical cancer worldwide. *J Pathol*, 189, 12-9.
- WANG, S. X., ZHANG, X. S., GUAN, H. S. & WANG, W. 2014. Potential Anti-HPV and Related Cancer Agents from Marine Resources: An Overview. *Mar Drugs*, 12, 2019-35.
- WANG, Y., COULOMBE, R., CAMERON, D. R., THAUVETTE, L., MASSARIOL, M. J., AMON, L. M., FINK, D., TITOLO, S., WELCHNER, E., YOAKIM, C., ARCHAMBAULT, J. & WHITE, P. W. 2004. Crystal structure of the E2

- transactivation domain of human papillomavirus type 11 bound to a protein interaction inhibitor. *J Biol Chem*, 279, 6976-85.
- WATTS, K. J., THOMPSON, C. H., COSSART, Y. E. & ROSE, B. R. 2002. Sequence variation and physical state of human papillomavirus type 16 cervical cancer isolates from Australia and New Caledonia. *Int J Cancer*, 97, 868-74.
- WILSON, R., FEHRMANN, F. & LAIMINS, L. A. 2005. Role of the E1(Λ)E4 Protein in the Differentiation-Dependent Life Cycle of Human Papillomavirus Type 31. *J Virol*, 79, 6732-40.
- WOYTEK, K. J., RANGASAMY, D., BAZALDUA-HERNANDEZ, C., WEST, M. & WILSON, V. G. 2001. Effects of mutations within two hydrophilic regions of the bovine papillomavirus type 1 E1 DNA-binding domain on E1-E2 interaction. *J Gen Virol*, 82, 2341-51.
- YANG, J., YAN, R., ROY, A., XU, D., POISSON, J. & ZHANG, Y. 2015. The I-TASSER Suite: protein structure and function prediction. *Nat Methods*, 12, 7-8.
- YIM, E. K. & PARK, J. S. 2005. The role of HPV E6 and E7 oncoproteins in HPV-associated cervical carcinogenesis. *Cancer Res Treat*, 37, 319-24.
- ZEKRI, A. R., BAHNASSY, A. A., SEIF-ELDIN, W. M., ALAM EL-DIN, H. M., MADBOULY, M. S., ZIDAN, A. Z., EL-HOSHY, K., EL-RAMLY, A. & ABDEL-HAMID, N. A. 2006. Role of human papilloma virus (HPV) in common and genital warts and its relation to P53 expression. *J Egypt Natl Canc Inst*, 18, 117-24.
- ZUNA, R. E., SIENKO, A., LIGHTFOOT, S. & GAISER, M. 2002. Cervical smear interpretations in women with a histologic diagnosis of severe dysplasia: factors associated with discrepant interpretations. *Cancer*, 96, 218-24.
- ZUR HAUSEN, H. 2000. Papillomaviruses causing cancer: evasion from host-cell control in early events in carcinogenesis. *J Natl Cancer Inst*, 92, 690-8.

APPENDIX



จุฬาลงกรณ์มหาวิทยาลัย
CHULALONGKORN UNIVERSITY

Preparation for SDS-PAGE

Stock reagents

30% Acrylamide, 0.8% bis-acrylamide, 100 ml

Acrylamide 29.2 g

N,N'-methylene-bis-acrylamide 0.8 g

Adjust volume to 100 ml with distilled water

1.5 M Tris-HCl pH 8.8

Tris (hydroxymethyl)-aminomethane 18.17 g

Adjust pH to 8.8 with 1 M HCl

Adjust volume to 100 ml with distilled water

2.0 M Tris-HCl pH 8.8

Tris (hydroxymethyl)-aminomethane 24.20 g

Adjust pH to 8.8 with 1 M HCl

Adjust volume to 100 ml with distilled water

0.5 M Tris-HCl pH 6.8

Tris (hydroxymethyl)-aminomethane 6.06 g

Adjust pH to 6.8 with 1 M HCl

Adjust volume to 100 ml with distilled water

1.0 M Tris-HCl pH 6.8

Tris (hydroxymethyl)-aminomethane 12.10 g

Adjust pH to 6.8 with 1 M HCl

Adjust volume to 100 ml with distilled water

Solution B (SDS-PAGE)

2.0 M Tris-HCl pH 8.8 75 ml

10% (w/v) SDS 4 ml

Distilled water 21 ml

Solution C (SDS-PAGE)

1.0 M Tris-HCl pH 8.8 50 ml

10% (w/v) SDS 4 ml

Distilled water 46 ml

SDS-PAGE**15% Separating gel**

30% Acrylamide solution 5.0 ml

Solution B 2.5 ml

Distilled water 2.5 ml

10% (w/v) $(\text{NH}_4)_2\text{S}_2\text{O}_8$ 50 μl

TEMED 10 μl

5.0% Separating gel

30% Acrylamide solution 0.67 ml

Solution C 1.0 ml

Distilled water 2.3 ml

10% (w/v) $(\text{NH}_4)_2\text{S}_2\text{O}_8$ 30 μl

TEMED 5.0 μl

5X Sample Buffer

1 M Tris-HCl pH 6.8 0.6 ml

50% Glycerol 5.0 ml

10% (w/v) SDS 2.0 ml

2-mercaptoethanol 0.5 ml

Distilled water 0.9 ml

Electrophoresis buffer, 1 liter

Tris (hydroxymethyl)-aminomethane 3.03 g

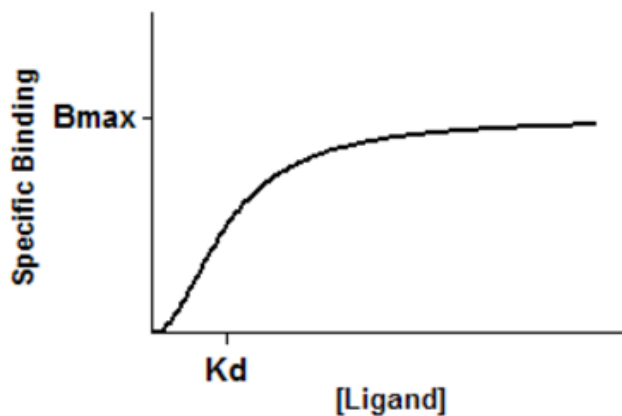
Glycine 14.40 g

SDS 1.0 g

Graphpad Prism Equation

Equation: One site -- Specific binding with Hill slope

Model: $Y = B_{max} * X^h / (K_d^h + X^h)$



Interpret the parameters

B_{max} is the maximum specific binding in the same units as Y.

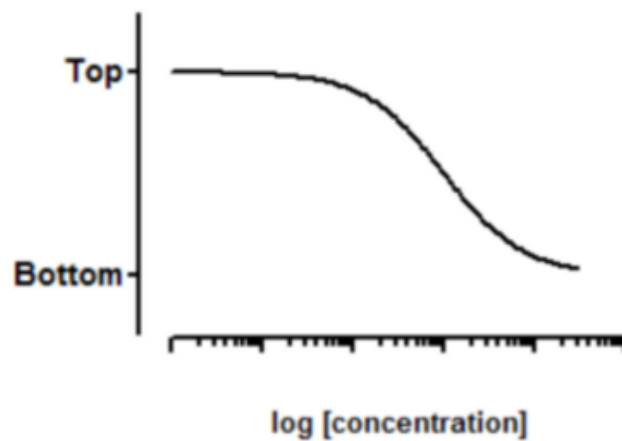
K_d is the radioligand concentration needed to achieve a half-maximum binding at equilibrium.

h is the Hill slope. It equals 1.0 when a monomer binds with no cooperativity to one site. When it is greater than 1.0, this happens when the receptor or ligand has multiple binding sites with positive cooperativity. The Hill slope is less than zero

when there are multiple binding sites with different affinities for ligand or when there is negative cooperativity.

Equation: log(agonist) vs response (three parameters)

Model: $Y = \text{Bottom} + (\text{Top} - \text{Bottom}) / (1 + 10^{-(X - \text{LogIC}_{50})})$



Interpret the parameters

IC_{50} is the concentration of agonist that gives a response half way between Bottom and Top. Top and Bottom are plateaus in the units of the Y axis.



VITA

Mr. Worrapon Kantang was born on August 18, 1988 in Chaiphum. He graduated with the degree of Bachelor of Allied Health Science in 2010. He has studied the degree of Master of Science at the Department of Biochemistry, Chulalongkorn University since 2012. In 2014, he presented a poster entitled “Elucidation of the binding conformations and interactions between small peptide inhibitors and human papillomavirus 16 protein” at 26th 40 Annual Meeting of the Thai Society for Biotechnology and International Conference on November 26-28, 2014. His work on the topic of “Design of peptides as inhibitors of human papillomavirus 16 transcriptional regulator E1-E2” has been accepted for a publication in *Chemical Biology & Drug Design* journal.